Geomorphology xxx (2016) xxx–xxx

Contents lists available at ScienceDirect

Geomorphology

journal homepage: www.elsevier.com/locate/geomorph

The problem of predicting the size distribution of sediment supplied by hillslopes to rivers

Leonard S. Sklar [a,*], Clifford S. Riebe [b], Jill A. Marshall [a,c], Jennifer Genetti [a], Shirin Leclere [a], Claire L. Lukens [b], Viviane Merces [a]

[a] Department of Earth & Climate Sciences, San Francisco State University, United States
[b] Department of Geology and Geophysics, University of Wyoming, United States
[c] Department of Earth and Planetary Science, University of California, Berkeley, United States

ARTICLE INFO

Article history:
Received 13 December 2015
Received in revised form 2 May 2016
Accepted 3 May 2016
Available online xxxx

Keywords:
Sediment supply
Hillslope weathering
Particle size reduction
Geomorphic transport law

ABSTRACT

Sediments link hillslopes to river channels. The size of sediments entering channels is a key control on river morphodynamics across a range of scales, from channel response to human land use to landscape response to changes in tectonic and climatic forcing. However, very little is known about what controls the size distribution of particles eroded from bedrock on hillslopes, and how particle sizes evolve before sediments are delivered to channels. Here we take the first steps toward building a geomorphic transport law to predict the size distribution of particles produced on hillslopes and supplied to channels. We begin by identifying independent variables that can be used to quantify the influence of five key boundary conditions: lithology, climate, life, erosion rate, and topography, which together determine the suite of geomorphic processes that produce and transport sediments on hillslopes. We then consider the physical and chemical mechanisms that determine the initial size distribution of rock fragments supplied to the hillslope weathering system, and the duration and intensity of weathering experienced by particles on their journey from bedrock to the channel. We propose a simple modeling framework with two components. First, the initial rock fragment sizes are set by the distribution of spacing between fractures in unweathered rock, which is influenced by stresses encountered by rock during exhumation and by rock resistance to fracture propagation. That initial size distribution is then transformed by a weathering function that captures the influence of climate and mineralogy on chemical weathering potential, and the influence of erosion rate and soil depth on residence time and the extent of particle size reduction. Model applications illustrate how spatial variation in weathering regime can lead to bimodal size distributions and downstream fining of channel sediment by down-valley fining of hillslope sediment supply, two examples of hillslope control on river sediment size. Overall, this work highlights the rich opportunities for future research into the controls on the size of sediments produced on hillslopes and delivered to channels.

1. Introduction

River channels are connected to surrounding hillslopes by sediment. In low-order, upland channels, the bed material and sediment flux are composed almost entirely of rock particles originally produced on hillslopes by physical and chemical weathering processes acting on bedrock. The size distribution of sediments supplied by hillslopes to channels is a key boundary condition that regulates channel morphodynamics, including channel slope and shape, rates of incision into bedrock, and habitat value for a wide range of organisms (Wohl, 2004; Sklar and Dietrich, 2004; Riebe et al., 2014). Thus, the systematic trends in morphology and process that characterize channel networks (Montgomery and Buffington, 1997; Gomi et al., 2002) may reflect spatial variations in the hillslope weathering processes that produce and deliver sediments to rivers. Weathering, in turn, is ultimately controlled by the landscape-scale boundary conditions of lithology, climate, and tectonics (Stallard, 1995; Brantley and Lebedeva, 2011), making the size of sediments supplied by hillslopes to channels an essential link in understanding how landscapes evolve. Despite its importance, there are few data and limited theory to inform predictions of the sediment size supplied to channels in either natural or modeled landscapes (National Research Council, 2010). The purpose of this paper is to propose a new research direction focused on a series of fundamental questions: What controls the size distribution of sediments produced on hillslopes? How does size evolve as particles travel through the hillslope weathering engine? Can we develop a general model for predicting variations in particle size distributions supplied to rivers at the landscape scale?

Much is known about how the size of sediments carried by rivers controls channel morphodynamics. For example, channel slope can be set by bed material grain size in both alluvial (Howard, 1980) and

* Corresponding author.
E-mail address: leonard@sfsu.edu (L.S. Sklar).

http://dx.doi.org/10.1016/j.geomorph.2016.05.005
0169-555X/

bedrock channels (Sklar and Dietrich, 2006; Johnson et al., 2009). River incision into bedrock, which sets the pace of landscape evolution, is regulated by the tools and cover effects of coarse sediment (Sklar and Dietrich, 2004; Turowski and Richenmann, 2009). These effects largely depend on two variables: the fraction of the total sediment load carried as bedload, and the characteristic bedload particle size. The effects of sediment size on bedrock incision help explain the width of bedrock channels (Finnegan et al., 2007; Nelson and Seminara, 2011), the propogation of knickpoints along channel profiles (Cook et al., 2013), the response of landscapes to accelerated fault motion (Cowie et al., 2008) and the long-term persistence of mountain ranges (Egholm et al., 2013). At the time scale of individual floods, the sediment size distribution influences the frequency and magnitude of bedload sediment transport (Lenzi et al., 2004), and the hydraulic roughness, which regulates flow depth for a given discharge (Rickenmann and Recking, 2011; Johnson, 2014). At longer time scales, sediment size also regulates alluvial channel cross-sectional and planform geometry (Doyle and Shields, 2000; Church 2006; Parker et al., 2007). Bed sediment size also influences aquatic ecosystems, including the occurrence of spawning habitat for salmonids (Riebe et al., 2014). The size distribution of sediment in rivers is also a key response variable for gauging the impacts of human land use on river systems, such as armoring of channels (Vericat et al., 2006) and filling of pools with fine sediments (Rathburn and Wohl, 2003) downstream of dams.

Whereas linkages between sediment size and in-channel processes have been widely studied, much less work has been done on understanding how sediment size variation through channel networks is influenced by hillslope sediment supply. A reach of channel receives sediments that were originally produced on hillslopes distributed throughout the upstream catchment area. The sizes of sediments supplied to the reach include the inputs from adjacent hillslopes and an integrated mixture of sizes produced upstream, weighted by the erosion rates of source hillslopes, and modified by particle abrasion and sorting in transport. Much work has focused on how size reduction by abrasion and sorting by size-selective transport may explain the characteristic downstream fining of bed material (Paola et al., 1992; Kodama, 1994; Miller et al., 2014; Menting et al., 2015). However, these processes are secondary controls on particle size because they can only modify the original size distribution that hillslopes provide to the channel network. Moreover, at the time scale at which landscapes evolve, size-selective transport is only effective where accommodation space exists to permit long-term deposition of less-mobile coarser particles (Ferguson et al., 1996), which is rare in the upland portions of tectonically active landscapes. Furthermore, particle abrasion can enhance the importance of local supply from hillslopes in controlling the size and abundance of the coarse fraction of the size distribution. This is because abrasion, which produces sand- and silt-sized fragments from coarser particles, has the greatest effect on particles that have traveled the longest distances. Thus, where the effects of abrasion are significant, the coarse river-bed material may dominantly reflect the size distribution of the fresh supply from local hillslopes and low-order tributaries (Heller et al., 2001; Sklar and Dietrich, 2006). This suggests that trends in sediment size through channel networks, such as downstream fining, could reflect trends in the size of hillslope sediment supply, due to spatial variation in the geologic and climatic factors that control hillslope weathering.

Only a handful of studies have directly compared the size distributions of sediments in channels and adjacent hillslope sources. Krumbein and Tisdel (1940) found that distributions of weathered rock fragments shed from outcrops of gneiss and granite bedrock could be fit with exponential distributions similar to those observed in stream sediments elsewhere. Ibbeken (1983) also found an exponential fit to hillslope sediment distributions but adjacent channel size distributions were bimodal. Wolcott (1988) compared size distributions along transects from ridge to channel and found bimodal distributions in the channel and near-channel hillslope locations, but not near ridges. These observations suggest that the commonly observed 'gap' in the size distribution of stream sediments (Smith et al., 1997; Radoane et al., 2008) could result from weathering process on hillslopes that produce a bimodal supply to channels. Other studies have implicitly linked hillslope conditions to channel sediment size, such as positive correlations observed between bed material size and the durability of underlying bedrock (Miller, 1958; Attal and Lavé, 2006; O'Connor et al., 2014).

Recent recognition of the crucial role of sediment in bedrock river incision has motivated renewed efforts to identify landscape-scale controls on the sediment size produced on hillslopes. Working in a granitic catchment draining the eastern flanks of the High Sierra, in California, Riebe et al. (2015) used geochemical tracing techniques to compare the elevations of hillslope source areas of coarse gravel and finer material sampled from the stream bed. They found that, on average, gravel source areas have higher elevations, and are colder, steeper, less vegetated, and eroding more rapidly than the source areas of finer sediment (Fig. 1A). Analyzing particle size distributions in soil pedons, Marshall and Sklar (2012) found a similar correlation between elevation and rock fragment size and abundance, along three transects with varying precipitation (Fig. 1B). Exploiting a spatial gradient in hillslope erosion rates, Attal et al. (2015) found that the size and abundance of rock fragments in soils are greater on more rapidly eroding hillslopes, and greater still in the debris at the base of steep bare bedrock slopes (Fig. 1C). Studying the variation of bed material size in the Marysandi River of Nepal, Attal and Lavé (2006) concluded that a downstream coarsening trend could be explained by a downstream increase in the supply from hillslopes of coarse landslide-derived sediments, and a corresponding decrease in the supply of finer glacially-derived sediment. Finally, investigating accelerated slip along normal faults in the Appenine mountains of Italy, Whittaker et al. (2008, 2010) documented a bimodal size distribution of sediments delivered to coastal basins, with the coarse mode supplied by landslides in the zone of rapid erosion.

These studies suggest that there may be general trends in the size of sediments produced on hillslopes and supplied to channels, which can be predicted from knowledge of landscape-scale factors such as lithology, climate, and erosion rate. Here we propose the hypothesis that these factors can be used in a simple numerical model (sensu the "geomorphic transport laws" of Dietrich et al., 2003) to predict the landscape-scale variation in the sediment size supplied to channels. The corresponding null hypothesis is that the variability is too large to permit accurate predictions, that every catchment is unique. A successful model would use as inputs simple metrics for each driving factor, capture their influence on the fundamental physical and chemical processes that produce and modify sediment particles on hillslopes, and generate predictions that could be tested in the field. Such a model would help us answer key questions about the connections between hillslopes and channels, such as: Does downstream fining of bed material reflect down-valley fining of hillslope sediment supply? Are bimodal sediment size distributions in channels the result of weathering processes on hillslopes? Do different size fractions on channel beds represent distinct geomorphic settings on the source hillslopes in the upstream catchment?

We pose these questions from the vantage point of a coarse-bedded river in an eroding mountainous landscape, with direct connection to adjacent hillslopes. To understand the size of sediments the river receives, we need to look upslope and consider the path that particles traverse on their journey to the channel, which begins in unweathered bedrock and passes through the hillslope weathering engine. Along this path the particle passes through many other potential vantage points, because the evolution of particle size on hillslopes is also important for understanding a diverse set of subjects, including hillslope hydrology, biogeochemical cycling, and human land-use, all of which are influenced by the size distribution of hillslope regolith (Gómez-Plaza et al., 2001; Silver et al., 2000; Montgomery, 2007; Maher and Chamberlain, 2014). Thus, solving this problem will require drawing

Please cite this article as: Sklar, L.S., et al., The problem of predicting the size distribution of sediment supplied by hillslopes to rivers, Geomorphology (2016), http://dx.doi.org/10.1016/j.geomorph.2016.05.005

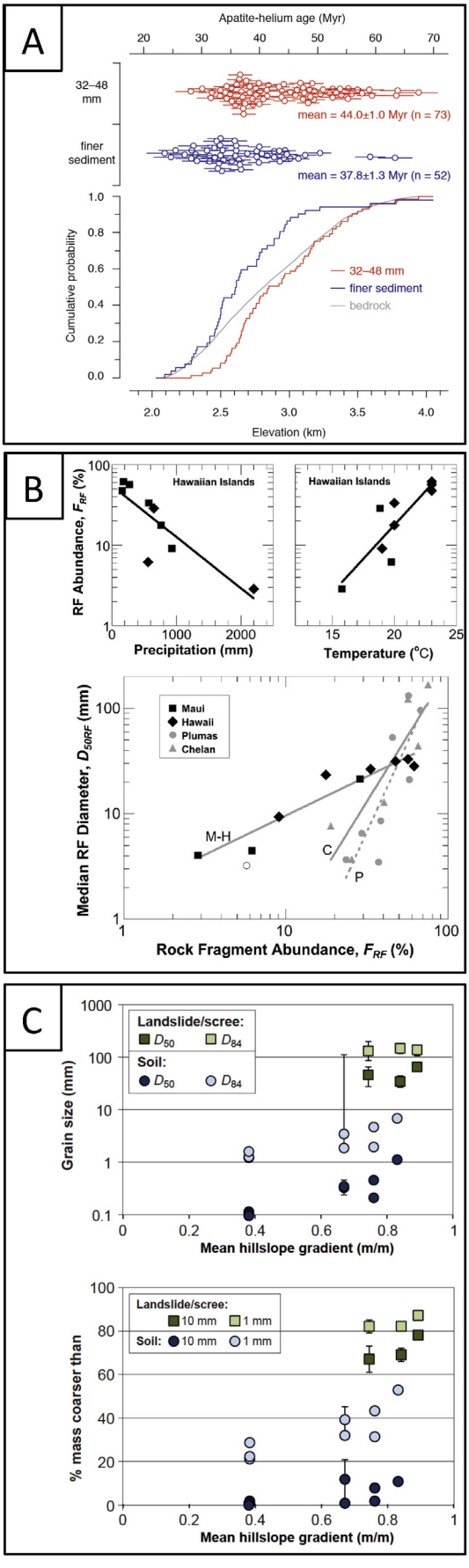

on the techniques and insights of many disciplines. It will also help to illuminate how the dynamics of weathering on hillslopes are expressed in the sediments passing through the river network, which in turn regulate the evolution of landscapes.

2. Dependent variables: What we want to predict

To our knowledge, no study has successfully predicted how the size distribution of sediment supplied to the channel network varies across a landscape. However, it is still possible to model the effects of input sediment sizes on bedload and river incision into bedrock. One approach is to first assume a functional form and then assign values to the parameters that control the central tendency and spread of the size distribution. For example, Egholm et al. (2013) used a fractal distribution to model sediment input by landslides, while Sklar et al. (2006) used a log-normal distribution to represent sediment delivered by all processes (Fig. 2). Another approach, is to use empirical data to quantify model inputs. For example, Attal and Lavé (2006) used measured size distributions from landslides, glacial moraines and terraces to model sediment inputs in their analysis of downstream fining (Fig. 2).

Although these approaches were able to highlight the potentially strong influence of sediment supply on bed material size and rates of river incision, they are not generalizable across diverse landscapes because they do not incorporate a mechanistic understanding of how factors such as lithology, climate and tectonics influence the processes that produce, modify and deliver sediments to channels. To achieve this broader goal, we need a general model that in qualitative terms can be written as

$$P(D) = f(Lithology, Climate, Biology, Tectonics, Topography) \quad (1)$$

where $P(D)$ is the distribution of particle diameters (D) by mass. Ideally, the model would predict the complete size distribution, i.e. the mass fraction P for every discrete size D, without any assumptions about the shape of the distribution (i.e., whether it is log-normal, exponential, or fractal). The model should be flexible enough to capture the diverse influences of the independent variables over a wide range of possible outcomes, including bimodal distributions and any of the curves shown in Fig. 2. Predicted distributions could then be compared with field measurements and theory for different sources and settings. In practice, comparisons with field data are likely to use statistics that quantify the central tendency, the spread, and partitioning between coarse and fine modes of the distributions. Identifying what we want to predict is the easy part of translating Eq. (1) into a working model. The far greater challenge is identifying the relevant independent variables and quantifying their influence.

3. Independent variables: Landscape-scale controls

Many factors influence the particle size distribution of sediment supplied from hillslopes to channels. On the right hand side of Eq. (1) we list five categories of landscape-scale factors that are likely to regulate sediment production on hillslopes. Ideally, our model would integrate the effects of the most important factors in each category. In this section we consider each category in turn, with the goal of identifying the most important and readily measurable variables that might serve as

Fig. 1. Published evidence for spatial trends in the size of sediments supplied to channels by hillslopes. (A) Source elevations of coarse gravel are significantly higher than sources of finer sediments, as revealed by geochemical tracers, Inyo Creek, California (Riebe et al., 2015). (B) Soil rock fragment (RF) abundance varies with precipitation and temperature across climosequence in Hawaii (Chadwick et al., 2003); rock fragment median size correlates with RF abundance in Hawaii and two elevations transects in California and Washington (Marshall and Sklar, 2012). (C) Size and abundance of rock fragments varies with hillslope gradient on hillslopes supplying sediment to the Feather River, California (Attal et al., 2015), where steepness varies along a spatial gradient in erosion rates due to accelerated baselevel lowering (Riebe et al., 2004; Hurst et al., 2012).

independent variables in a predictive model. We draw on new and previously published datasets to illustrate how sediment size distributions are influenced by factors that fall into the categories of Eq. (1).

3.1. Lithology

Sediment particles delivered to channels originate from bedrock underlying adjacent hillslopes. Hence, lithology (i.e., the physical and chemical characteristics of the bedrock) should be an important intrinsic regulator of the sizes delivered to channels. There are at least five distinct lithologic factors that might play an important role. First is the inherited particle size distribution of some clastic lithologies, such as conglomerates, sandstones, and volcanic breccias. These rock types are composed of particles deposited in the past by water, wind, and volcanic eruptions and thus have a tendency to produce particle size distributions that are inherited from the original distribution of clast sizes within the rock. This is illustrated in the outcrop and eroded debris of conglomerate shown in Fig. 3A. Similarly, in crystalline rocks, the size distribution of individual mineral grains will influence the particle size distribution that results from rock disaggregation due to chemical weathering. A third lithologic factor is the spacing of discontinuities such as bedding planes and joint sets, which can govern the maximum size of particles produced by weathering and erosion on slopes. In Fig. 3B, the particle sizes shed by erosion of a basalt flow are similar to the spacing between the joints in the outcrop. A fourth lithologic factor is mineralogy, and the susceptibility to chemical dissolution of the various mineral phases present in the rock. For example, a lithology might be more susceptible to disaggregation into mineral-sized particles if it has abundant biotite – which can expand during weathering and thus shatter surrounding rock along grain boundaries. The propensity of biotite-rich granitic bedrock to break down into mineral-sized fragments is illustrated in the outcrop shown in Fig. 3C. A fifth factor is intact rock strength, which varies over four orders of magnitude (Sklar and Dietrich, 2001). All else equal, we expect the sizes of sediment produced on slopes to increase with rock strength because stronger bedrock can better resist the propagation of fractures under stresses that arise from many sources, including topographic overburden, the growth of tree roots, and the development of ice lenses. This may help explain the observation that rock fragment size and abundance in gopher mounds scales with the mechanical strength of the underlying bedrock across three different lithologies (Fig. 4).

As a first step toward developing a predictive model of sediment size, we suggest that the five lithologic factors outlined above could be captured in the parameterization of two input variables. The first input variable combines the inherited-particle and mineral-grain size distributions, and the spacing of joints and bedding planes, into a probability distribution of latent sizes, $P(L)$, in the unweathered rock, where L has dimensions of length. In our formulation, the central tendency of $P(L)$ either reflects the inherited grain size distribution (e.g., for sedimentary bedrock) or scales with intact rock strength (σ_T). The second input variable is the susceptibility to weathering of minerals within the bedrock, expressed simply as the mass fraction of soluble minerals, F_{SM}, or an assemblage of values reflecting the concentrations of multiple minerals and their rate constants of weathering reactions (Ferrier and Kirchner, 2008).

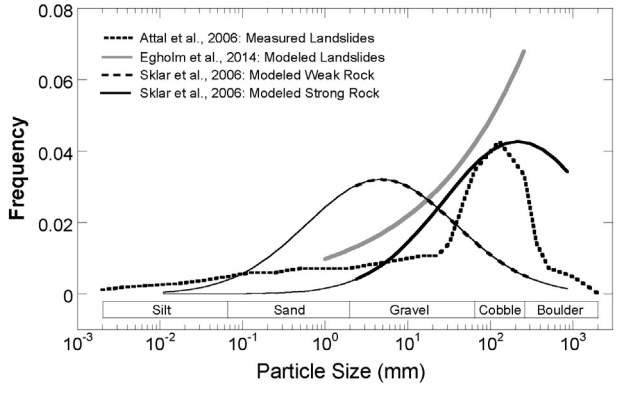

Fig. 2. Particle size distributions used in previous modeling studies that explored the effect of hillslope sediment supply on bed material size and rates of river incision into bedrock.

3.2. Climate

Sediment created from bedrock on hillslopes is exposed to corrosive waters and temperature fluctuations that reduce particle sizes via mineral dissolution and fracturing. The through-flow of water and the range of temperature variations on a hillslope are ultimately set by climate. Thus climatically driven differences in chemical and physical weathering should regulate the reduction of sediment sizes on the journey from bedrock to the stream channel. Wetter and warmer conditions should favor chemical weathering and thus the delivery of relatively fine-grained sediments to the channel due to the tendency of chemical processes to disaggregate rock at the scale of individual mineral grains. Conversely, drier and colder conditions should favor physical weathering and thus the delivery of coarser sediment due to the tendency of physical processes to break rock down at the scale of joints sets and bedding planes.

We suggest that climatically-driven differences in the relative importance of physical and chemical weathering may be a dominant regulator of differences in sediment production on hillslopes. Moreover, we propose that it can be captured in a predictive model in the parameterization of average temperature and precipitation. This is corroborated by observations from several field sites, including the Inyo Creek catchment (Figs. 1A, 3G) of Riebe et al. (2015). There, as shown in Fig. 5, we find that coarser sediments are preferentially produced at higher elevations, which are also exposed on average to colder temperatures that presumably favor physical over chemical weathering. Thus temperature may be an important explanatory variable in the distribution of sediment sizes produced on hillslopes. The role of precipitation is highlighted across a climosequence of soils in Hawaii (Chadwick et al., 2003), where the abundance of rock fragments (sediment particles >2 mm in diameter) was found to decrease rapidly with increasing average precipitation (Fig. 1B; Marshall and Sklar, 2012).

In focusing on average temperature and precipitation, we ignore, for now, the many other climatic factors that could influence sediment size distributions. This is a necessary simplification to allow for a tractable solution. Although the breakdown of rock may be influenced by temperature variability, via freezing and thawing, and by precipitation variability, via wetting and drying, we assume that these effects are subordinate to the first-order effects of differences in average temperature and precipitation.

3.3. Life

Organisms pervade virtually all climate zones across Earth's surface (Pedersen, 2000; Thomas and Dieckmann, 2002), and affect a wide range of geomorphic processes (Dietrich and Perron, 2006; Roering et al., 2010; Amundson et al., 2015). Hence, we should expect both flora and fauna to contribute to the production and modification of sediment particles on hillslopes. At the smallest scale, microbes mediate many of the chemical weathering reactions that break down rock (Newman and Banfield, 2002). At a larger scale, the roots of trees break rock apart by widening and extending pre-existing fractures (Fig. 3D) and by mixing rock and soil when rock-laden root-wads are overturned by tree-throw (Gabet and Mudd, 2010; Pawlik, 2013). Trees can also influence whether soils are even present, through feedbacks between lithology, weathering and ecosystem processes (Hahm et al., 2014; Marshall and Roering, 2014). Burrowing animals ranging in size from worms to wombats can convert rock to soil, and transport

Please cite this article as: Sklar, L.S., et al., The problem of predicting the size distribution of sediment supplied by hillslopes to rivers, Geomorphology (2016), http://dx.doi.org/10.1016/j.geomorph.2016.05.005

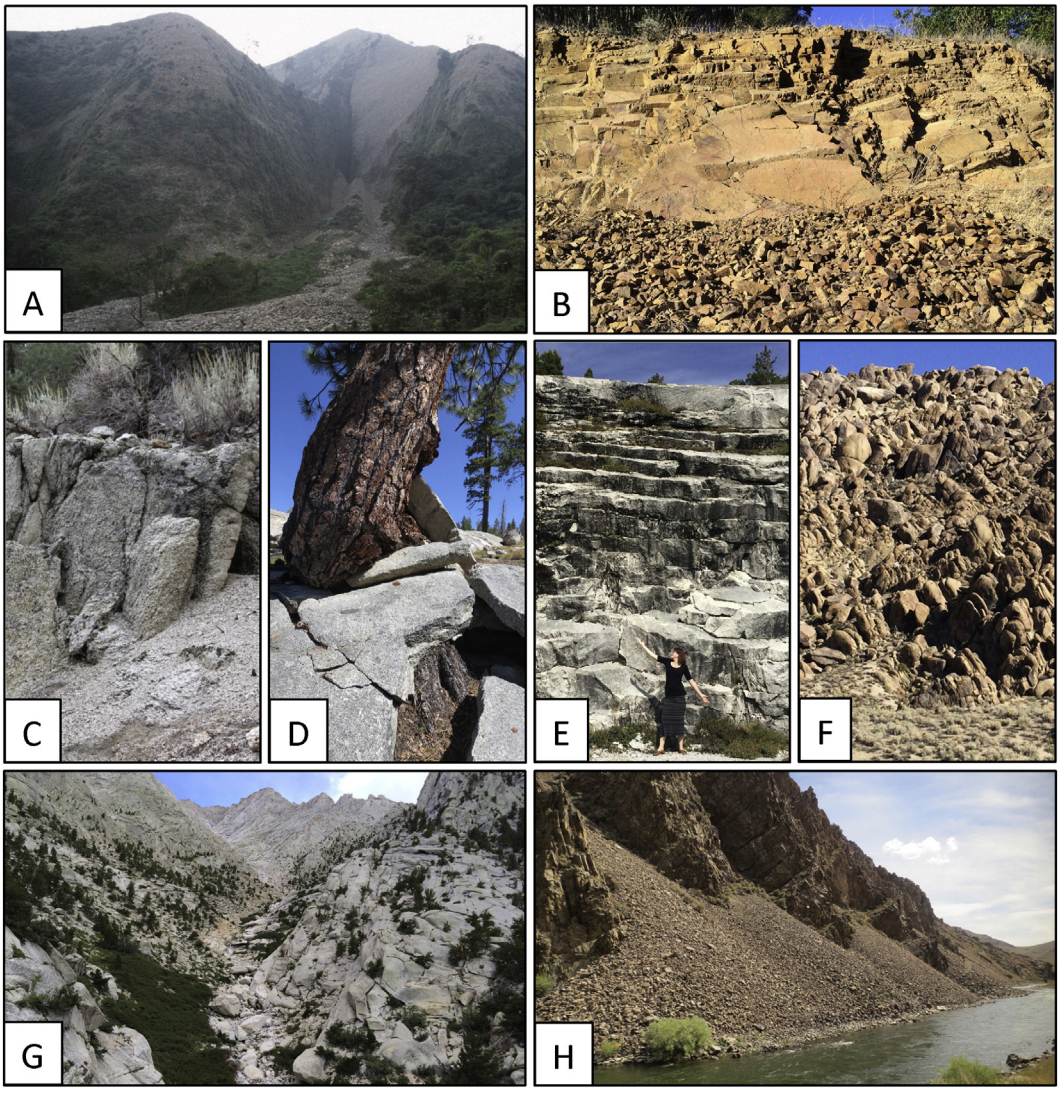

Fig. 3. Photographs illustrating sediment production and weathering on hillslopes (all sites in California, USA, unless noted). (A) Eroded particle size distribution inherited from conglomerate bedrock, Cholan formation, Wu River, Taichung County, Taiwan; (B) jointed outcrop shedding talus, Grizzley Peak Basalt, Wildcat Creek; (C) gruss produced by biotite weathering, Lone Pine Granodiorite, Inyo Creek; (D) granodiorite blocks fractured by tree roots, Stanislaus River; (E) sheet joints, Cathedral Peak Granodiorite, Tuolumne River; (F) granitic core stones, Alabama Hills; (G) production of large boulders from widely-spaced bedrock fractures, Whitney Granodiorite, Inyo Creek; (H) talus supplied directly to channel, Swauger Formation Quartzite, Salmon River, Idaho.

soil downslope (Gabet et al., 2003; Heimsath et al., 2000). Perhaps the most potent biotic agents today are humans (Hooke, 2000), who affect the size of sediment delivered to channels through road building, logging, and a host of other land uses.

Setting human impacts aside as a topic for another study, we now consider how the influence of organisms on hillslope sediment size might be parameterized in a simple model. One approach might use a variable to represent the frequency and intensity of biotic disturbance of bedrock, where for example coarser particles might be produced by forest ecosystems and finer particles by grasslands, all else equal. Another approach would consider the actions of individual species and their relative abundance. A more general approach would use bulk ecosystem measures such as surface biomass or primary productivity to scale the effects of organisms. These measures of biotic activity also scale with climatic variables, such as mean annual temperature and precipitation (e.g. Field et al., 1998), suggesting that in the simplest approach, the effects of life might be subsumed within the parameterization of climate. This is the approach we adopt here, although future work could expand on this first attempt for a more complete parameterization of the effects of life on hillslope sediment sizes.

3.4. Tectonics and erosion

Tectonics can influence the sizes of sediment produced in two main ways. First, tectonic stresses in the crust fracture bedrock as it is exhumed to the surface, influencing the distribution of latent sizes $P(L)$ delivered by bedrock exhumation to the base of the weathering engine. For example, in tectonically active areas, such as along convergent margins, pervasive fracturing in the upper crust may be the fundamental regulator of $P(L)$ due to slip on faults and deformation in surrounding blocks across all scales (Molnar et al., 2007). Meanwhile, in regions that lack significant faulting, such as granitic intrusions in arc settings that have been exhumed without significant deformation, $P(L)$ may be more closely linked to sheet jointing (Fig. 3E), which reflects the interaction of regional tectonic stresses and local topographic curvature (Martel, 2006). Thus we expect the central tendency, spread, and shape of $P(L)$ to be sensitive to tectonic forcing through its influence on stress and strain in the crust across a broad range of tectonic settings.

A second main way that tectonics can influence the sizes of sediment supplied to channels is by modulating the residence time of sediment on slopes. All else equal we expect sediment that passes through the

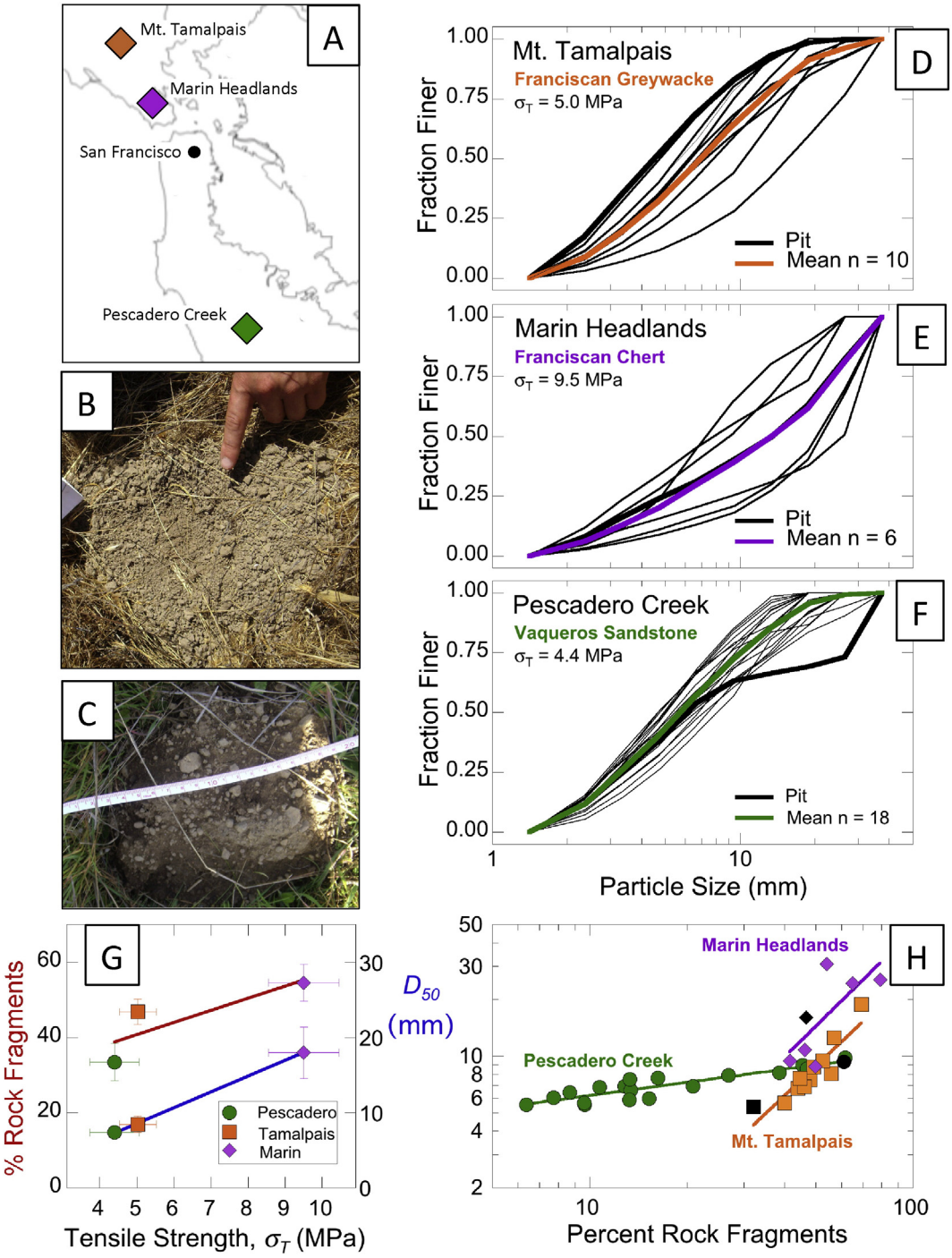

Fig. 4. Influence of rock strength on size and abundance of rock fragments in soil. We sampled soils delivered to the surface by burrowing gophers at three sites in Northern California underlain by distinct lithologies (A). Entire gopher mounds (B, C) were collected and sieved to obtain cumulative particle size distributions and mass fraction of rock fragments ($D < 2$ mm) (D, E, F). We also sampled one 50 cm deep pit at each site, and sampled relatively unweathered bedrock exposures for tensile splitting strength testing (ISRM, 1978). At each site, median rock fragment size correlates with rock fragment abundance (H). Across sites, both size and abundance of rock fragments correlate with bedrock tensile strength, σ_T (G).

weathering engine quickly to be coarser than sediment that passes through more slowly. Sediment residence time (R_t), calculated to first order as the ratio of the thickness of the weathering zone (H_w) to the erosion rate (E_r),

$$R_t = \frac{H_w}{E_r} \tag{2}$$

can be influenced by tectonics in two ways. First, tectonic uplift drives relative baselevel lowering of the channel network, which influences rates of channel incision and thus hillslope erosion. Second, the interaction of regional tectonic stresses and local topographic curvature sets the depth and pattern of opening mode stress in the shallow subsurface (Martel, 2006), inducing thicker weathering profiles under ridges in compressive regions and thinner weathering profiles under ridges in extensional regions (St. Clair et al., 2015). Thus tectonics can affect both the numerator and the denominator in Eq. (2).

Erosion rate is a straightforward input variable to represent tectonics in a model of hillslope grain size. A positive correlation between erosion rate and sediment size has been observed in two field studies where

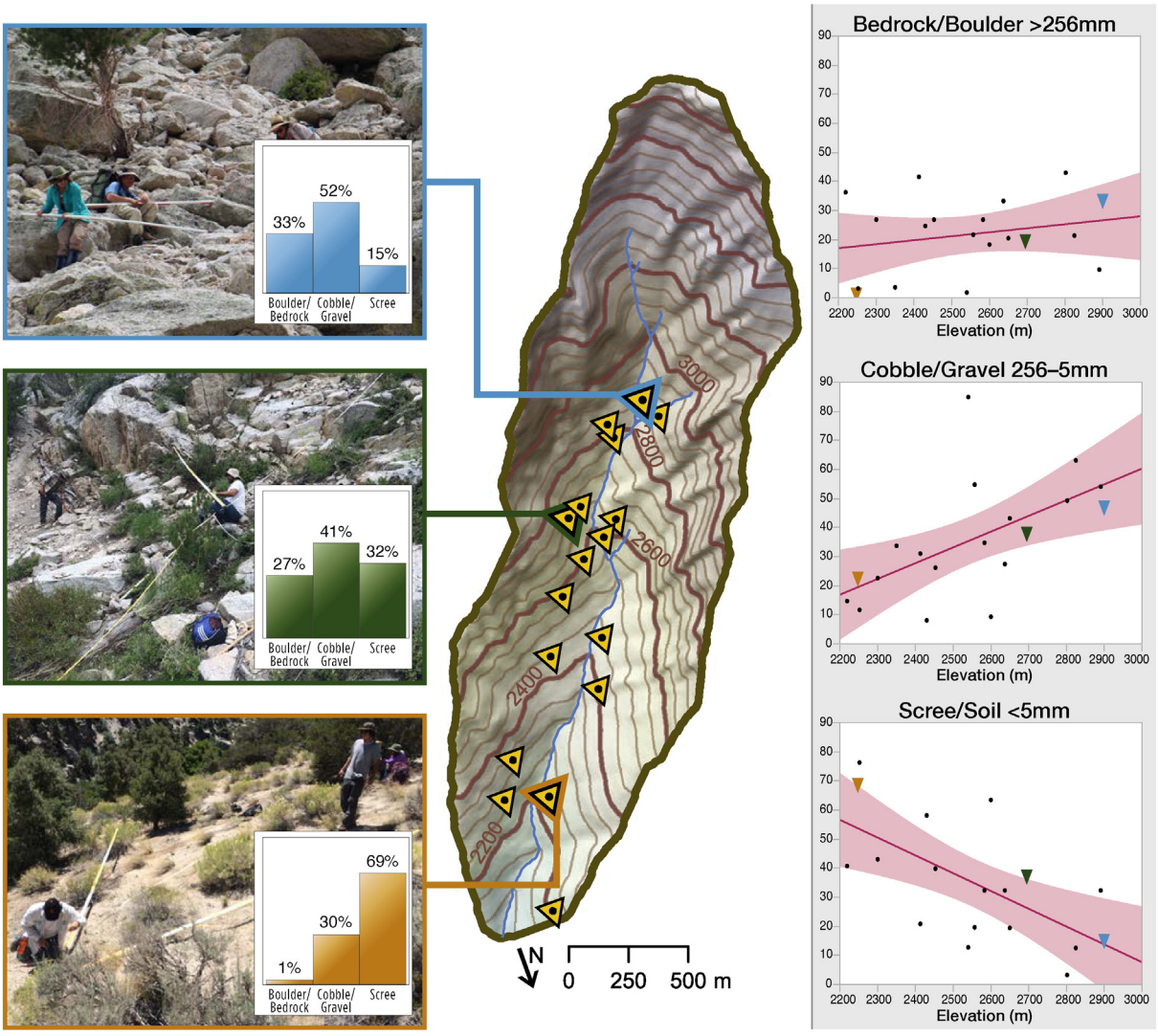

Fig. 5. Variation in hillslope surface particle size with elevation at Inyo Creek, High Sierra, California. Map shows 17 randomly-selected sites where we used point counts ($n = 100$; area = 100 m^2) to quantify the fraction of ground surface in three grain size bins: boulders ($D > 256$ mm), cobble/gravel (5 mm $< D <$ 256 mm), and soil/scree ($D < 5$ mm). Photos show three representative measurement locations illustrating changes in ground cover over a 700 m elevation range; inset histograms show local size distributions. The three scatterplots show variation of fraction in each size bin with elevation across all 17 sites. As elevation increases we find a significant ($p < 0.05$) decrease in soil/scree and increase in cobble/gravel, but no significant trend in boulder fraction.

spatial variation in erosion rate was measured with cosmogeneic nuclides, the Inyo Creek site of Riebe et al. (2015), and the Feather River site studied by Attal et al. (2015) and Riebe et al. (2000). At both of these sites, faster erosion rates also correlate with steeper hillslope gradients (Fig. 1C), suggesting that slope, or other topographic attributes, could be used to represent the influence of erosion rate.

3.5. Topography and geomorphic process regime

Topography results from the interaction of tectonics with lithology, climate and life, factors that regulate the efficiency of erosional processes; thus topography should integrate the influences of all four factors discussed above. For example, we might expect landscapes with stronger bedrock, colder climates, lower biomass and more rapid uplift rates to supply the coarsest sediments to channels. We would also expect such landscapes to be steeper, with narrower ridges, thinner or absent soils, and more frequent landslides. This suggests that the sediment size supplied to channels could be predicted directly from attributes of topography and the dominant geomorphic processes.

Hillslope gradient, or slope, is perhaps the best single topographic attribute to correlate to sediment size, with steeper slopes delivering coarser particles. For example, it is common to observe boulders delivered to channels from steep valley slopes (Howard, 1998) or from steep debris-flow-dominated tributaries (Webb et al., 1988). Attal et al. (2015) measured an increasing trend in the size and abundance of rock fragment in soils, scree and landslide debris, with steeper slopes in the transient landscape near the Feather River gorge in California (Fig. 1C). Whittaker et al. (2010) also documented coarser supply from steeper landslide-dominated slopes. However, hillslope gradients can reach a critical slope angle, beyond which erosion rates and possibly sediment sizes increase with no change in slope steepness (Roering et al. 1999).

Thus, slope alone may be insufficient to capture thresholds in dominant hillslope geomorphic process, which may better explain spatial variation in sediment size produced. For example, hillslope curvature, together with slope, can be used to distinguish deep-seated landslides from areas dominated by creep or shallow landsliding (Roering et al., 1999; Booth et al., 2013). We might expect that distinct sediment size distributions would be produced in each of these hillslope process regimes (Mackey and Roering, 2011). Other topographic attributes that might correlate with geomorphic process regime and hillslope sediment size include aspect, and distance downslope from the

Please cite this article as: Sklar, L.S., et al., The problem of predicting the size distribution of sediment supplied by hillslopes to rivers, Geomorphology (2016), http://dx.doi.org/10.1016/j.geomorph.2016.05.005

ridgeline (Fig. 6), because both will influence the amounts of water, heat energy, and time available to weather rock fragments on their journey to the channel.

4. The path from bedrock to river

So far we've considered each independent factor separately, at the largest and most general scale, and identified quantitative variables that could be used to represent them in a numerical model. While each of these variables may be important in distinct ways, the actual mechanisms that produce and modify sediment sizes on hillslopes will depend on their combined effects, which will differ depending on the local geomorphic processes. To better understand the mechanisms at work, and define functional relationships between the independent variables and hillslope sediment size, we now look more closely at the life stages of a particle, as it travels from unweathered bedrock through the hillslope weathering engine, to the channel (Fig. 7). A large variety of processes may influence the initial size of particles entering the hillslope surface environment and how those sizes are transformed by weathering and transport before delivery to the channel. Because we are primarily concerned with the outcome for sediment supply to channels, we focus here on the question: what are the factors that control whether a parcel of exhumed rock will survive the weathering process to contribute coarse rock fragments that move as bedload in the fluvial system?

There are at least four strategies by which a rock fragment might reach the channel in the coarse size fraction (i.e. gravel and coarser for the upland channels considered here). The first strategy is – start out large, so that even if weathering reduces the particle size significantly, the resulting size will still be in the coarse size fraction. Second, encounter a relatively weak weathering engine, where particle size is not greatly reduced before delivery to the channel. Third, spend only a short time in the weathering engine, so that even if weathering potential is high, the net effect of weathering on particle size is limited. Finally, bypass the weathering engine and reach the hillslope surface, or even the channel, directly from bedrock; these particles will stand the best chance of escaping the size-reducing effects of weathering to become coarse bed material in the channel. The following four sub-sections consider each of these four strategies in turn, with the goal of identifying the functional relationships and parameters that might capture these effects in a predictive model of hillslope sediment size.

4.1. Initial particle size distribution

Rocks arrive at the base of the critical zone having accumulated fractures from the tectonic stress fields encountered during exhumation (Molnar et al., 2007). Additional stresses arise with proximity to the surface, such as stresses due to differential topographic loading (Miller and Dunne, 1996; St. Clair et al., 2015). Joints commonly occur in ordered sets with two or three orientations, reflecting the normal and deviatoric components of the stress fields that caused the fracturing (Pollard and Aydin, 1988). Many lithologies have other characteristic patterns of jointing, for example rhythmic bedding sequences in sedimentary rocks, foliations in metamorphic rocks, and cooling joints in volcanic rocks. These patterns of discontinuities in the rock set the initial fragment size template that weathering mechanisms act on.

Rock masses can be characterized as assemblages of 3-dimensional blocks bounded by joints, where block volume (V_b) depends on the spacing between joints and the angles between the joint orientations. Where three joint sets of consistent spacing intersect, the characteristic block volume can be estimated as

$$V_b = \frac{S_1 S_2 S_3}{\sin\gamma_1 \sin\gamma_2 \sin\gamma_3} \tag{3}$$

where S_i and γ_i are the average spacing and orientations of the i^{th} joint set (Palmstrom, 2005). From Eq. (3) the characteristic median block diameter (D_b) can be estimated as

$$D_b = V_b^{1/3}. \tag{4}$$

In any given rock mass, block volume can be highly variable, with distributions that span two or more orders of magnitude due to variability in both spacing and orientation, the presence of additional randomly-oriented joints, and variability in the persistence or length of joints (Kim et al., 2007; Cai, 2011). Block volume distributions are often estimated from measurements of joint frequency measured along linear transects, scan lines, or bore holes (Blenkinsop, 1991; Gillespie et al., 1993; Wines and Lilly, 2002). We can use this approach to quantify the latent particle size distribution $P(L)$ in terms of joint spacing.

Two types of equations are commonly used to describe the distribution of spacings in jointed and faulted rock (Blenkinsop, 1991). These can be adapted to quantify the particle size distribution of rock fragments produced from bedrock. The first type is a negative exponential function, such as the Rosin-Rammler distribution (Rosin and Rammler, 1933),

$$P(>D) = e^{-(D/k)^n} \tag{5}$$

where $P(>D)$ represents the mass fraction that would be retained on a sieve of size D. The 'scale' parameter k controls the central tendency while the exponent n is a "shape" parameter that is the reciprocal of the spread of the distribution. Eq. (5) is an integral form of the Weibull distribution (Weibull, 1951),

$$P(D) = \frac{n}{k}(D/k)^{n-1} e^{-(D/k)^n} \tag{6}$$

which describes the probability density function of particle sizes by mass (Fig. 8a). Exponential distributions are derived from the assumption that the probability that fractures will intersect to form detachable fragments scales with a characteristic spacing related to k (Blenkinsop, 1991). The exponential distribution has been widely used to fit fracture spacing data as well as size distributions resulting from geophysical comminution processes in rock, including Mt. St. Helens rockslide debris (Glicken, 1996) and regolith sampled on the Moon (Martin and Mills, 1977). It was also used in early comparisons of hillslope and river sediments (Krumbein and Tisdel, 1940; Ibbeken 1983).

A second type of equation commonly used for rock fracture distributions is a power function that produces a fractal distribution, which for particle sizes can be written as

$$N(>D) = kD^{-D_F} \tag{7}$$

where N is the number of particles greater than size D, fractal dimension D_F is the slope of the cumulative distribution plotted in log-log space, and the pre-factor k is the value of N when $D = 1$. The corresponding particle size distribution by mass can be written as

$$P(D) = \frac{D^{3-(D_F+1)}}{\int_{D_{min}}^{D_{max}} D^{3-(D_F+1)} dD} \tag{8}$$

assuming spherical particles and a finite particle size range bounded by D_{min} and D_{max} (Fig. 8b). Power distributions have a theoretical basis in the assumption that fracturing produces a self-similar cascade of branching cracks, which determines the probability of joint intersection and fragment production (Turcotte, 1986). Fractal distributions have been fit to both joint and particle size distributions in a wide variety of settings, including impact debris (Grady and Kipp, 1987), fault gouge (Blenkinsop, 1991), volcanic breccia (Roy et al., 2012) and soils (Perfect, 1997). Fractal distributions have also been used to model

Please cite this article as: Sklar, L.S., et al., The problem of predicting the size distribution of sediment supplied by hillslopes to rivers, Geomorphology (2016), http://dx.doi.org/10.1016/j.geomorph.2016.05.005

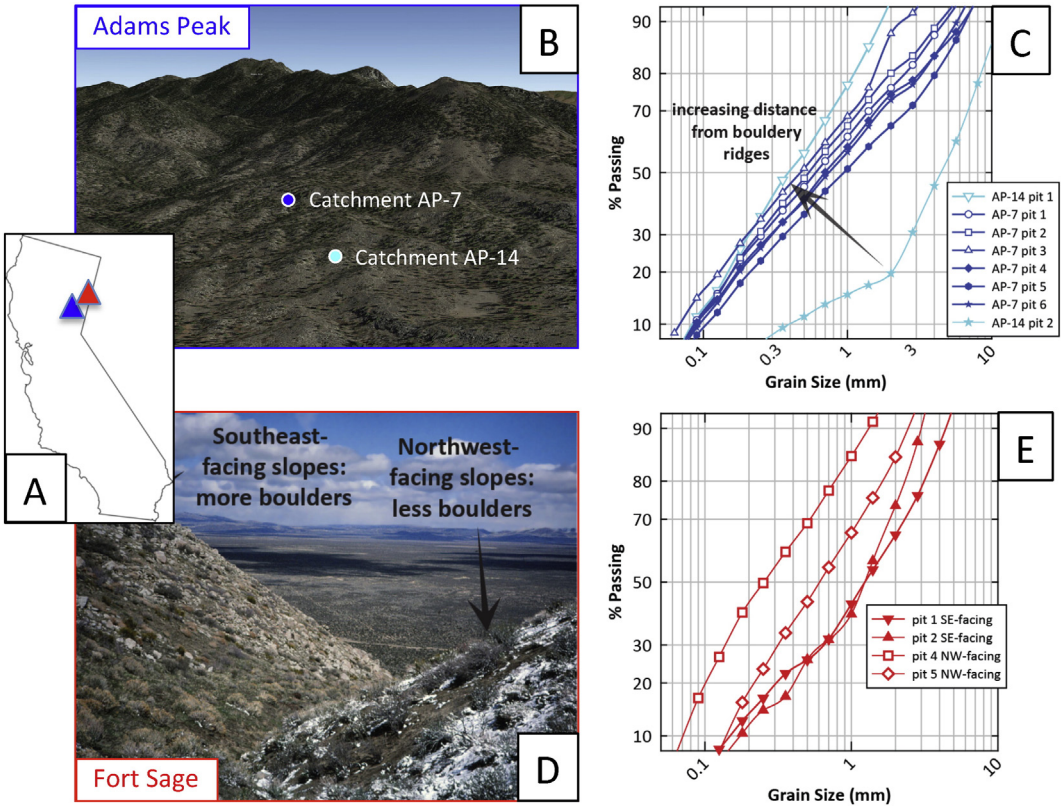

Fig. 6. Spatial trends in rock fragment size and abundance in soils at two sites in northeastern California (A) underlain by tonalite. Soil pits were dug to saprolite, sampled, sieved and weighed to obtain particle size distributions. Soils at Adams Peak site (B) are coarsest close to the boulder-dominated ridges, and become finer with increasing distance downslope (C). Soils at Fort Sage site (D) are coarser on southeast-facing slopes than on northwest-facing slopes (E); NW-facing slopes retain snow longer in spring, and have fewer surface boulders than SE-facing slopes.

coarse sediment supplied to rivers by landsliding (Egholm et al., 2013). The fractal dimension D_F of fractured rock generally varies between 2.0 and 4.0 (Blenkinsop, 1991), and is inversely correlated with average size (for a given value of k). Hence rocks subjected to stronger and longer-lasting tectonic deformation are likely to have higher D_F and produce finer particle size distributions. Power and exponential distributions differ primarily in the tails, with power generally over-predicting compared to exponential fits. To address this shortcoming, multi-fractal distributions are often used (Perfect, 1997), for example different values of D_F can be fit to the clay, silt and sand components of fine sediments in soils (Bittelli et al., 1999; Posadas et al., 2001).

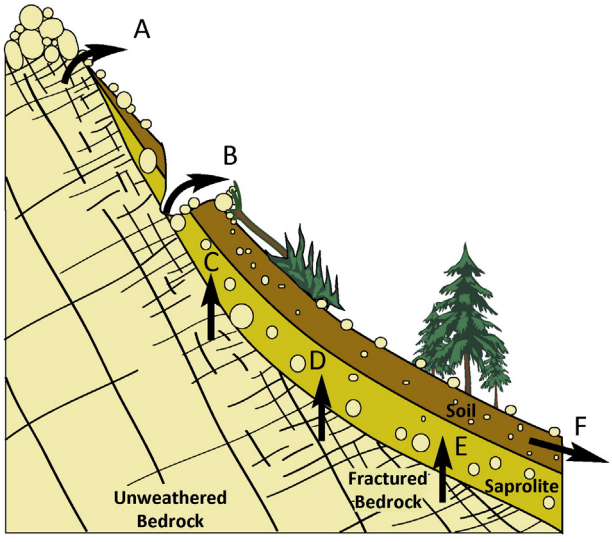

Fig. 7. Illustration of the paths rock particles can take from unweathered bedrock through the hillslope weathering zone to the channel. Initial size distribution is set by spacing of fractures inherited from depth and acquired near the surface. Rock particles can bypass soil weathering engine by being exhumed in bedrock outcrops (A) or by being lifted to the surface by tree throw (B). Within saprolite and mobile soil, rock fragment size may decline due to weathering, particularly if soils grow thicker and wetter in downslope direction (C, D, E). Coarse sediments supplied to the channel (F) include particles transported on the soil surface and within soil column.

Although the distribution of spacing between joints and other planes of weakness sets the template, the initial size distribution of rock fragments will also depend on the geomorphic processes that produce discrete transportable particles. In the simplest case, physical processes will extend existing fractures until fracture intersection detaches discrete blocks of rock. In this case, the initial size distribution of particles produced on bedrock hillslopes will be closely related the size distribution of joints in the fresh bedrock. The degree to which sediment production processes alter the initial fracture distribution, or create new fracture distributions, should also depend on the type and magnitude of the stresses acting on rock at the surface. For example, sheet or exfoliation joints (Fig. 3E) form parallel to curving rock surfaces due to tensile strain arising from regional compressive stresses (Martel, 2006; Ziegler et al., 2013). Sheets joints are most common in massive lithologies with high intact rock strength. When sheets are broken by fractures normal to the surface, large tabular blocks are often formed. In this case, we might expect the sheet thickness to set the short "c" axis of the initial blocks, depending on the spacing of the surface-normal joint sets. However, tabular blocks that are long, wide and thin are inherently prone to further development of cross-cutting fractures, so we might expect the sheet thickness to become the characteristic "b" axis size of sheet joint fragments after transport downslope.

Frost cracking is an example of a physical weathering mechanism that may modify the initial size distribution set by joint spacing. Rock fragment production by growth of segregation ice lenses in fractures is

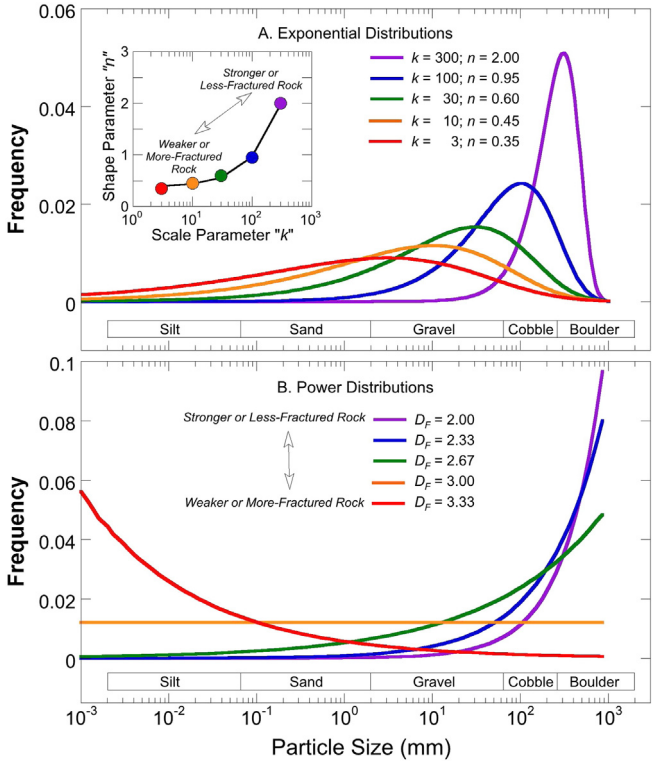

Fig. 8. Theoretical initial particle size distributions by mass. (A) Exponential distributions (Eq. (6)), with parameters k and n varied to illustrate expected widening of distribution with increased fracture density (inset). (B) Power distributions (Eq. (8)), for various values of fractal dimension D_F; scale parameter $k = 0.1$ mm for all curves.

important in landscapes where winter temperature (T) falls into the 'frost cracking window' of $-8\ °C < T < -3\ °C$ (Walder and Hallet, 1985; Hales and Roering, 2007; Murton et al., 2006). Frost cracking intensity is also influenced by proximity to liquid water (typically at lower, warmer depths in the rock), and the gradient in temperature with depth (Anderson et al., 2013; Girard et al., 2013; Marshall et al., 2015). Frost cracking is implicated in the production of talus (Fig. 3H), which commonly has a coarse and narrow size distribution (Hales and Roering, 2005; Jomelli and Francou, 2000). This could indicate that ice lenses preferentially grow in more widely spaced fractures, imposing a process-based characteristic size distribution. On the other hand, it may be that frost cracking is equally effective on more closely-spaced fractures, which where present lead to scree or finer particle size distributions with a less charismatic presence in the landscape.

Another process that may impose a characteristic size distribution is rock fragment production by trees. Tree root growth generates stresses capable of extending pre-existing fractures (Misra and Gibbons, 1996). Patterns of root growth into rock reflect the tree's need for water and for stability, especially where soil is thin or absent. Discrete rock fragments are formed gradually, as root growth drives fracture intersection, as well as catastrophically, when high winds overturn trees and cantilever torque acting through root wads exceeds the strength of fractured bedrock. The resulting fragment size distributions may reflect the tree height, and the size, density and spacing of roots of a given tree species (Roering et al., 2010), as well as environmental conditions such as soil depth and water availability (Zwieniecki and Newton, 1994). Other living organisms that produce rock fragments may also be size selective. For example, burrowing animals, which scrape at bedrock at the base of the soil column, are presumably limited to producing rock fragments smaller than some fraction of their body size (Fig. 4).

Chemical processes also initiate and extend fractures, and thus can detach rock fragments. For example, volumetric expansion during oxidative dissolution of ferrous minerals drives spheroidal weathering and formation of core stones in jointed coherent rock such as a granite and basalt (Fletcher et al., 2006). In dry climates with low erosion rates, the result can be slopes mantled with core-stone boulders (Fig. 3F; Oberlander, 1972; Whitney and Harrington, 1993), where the distribution of boulder sizes is related to the joint spacing in the unweathered bedrock. However, where bedrock and boulders are exposed at the surface, dissolution of the most soluble minerals can drive granular disintegration and release of sand- and pebble-sized gruss (Isherwood and Street, 1976). Thus, in arid and slowly eroding landscapes, even where hillslopes are mantled with boulders, the size of rock fragments reaching channels may primarily reflect the size of individual mineral grains, not the initial distribution of joint spacings.

4.2. Weathering intensity

Once rock fragments are detached, they begin their journey to the channel. How much their size is reduced on that journey depends on the type and intensity of weathering environments encountered along the way. Rock particles may already be altered by chemical weathering in the fractured bedrock and saprolite, but the most intense weathering is likely to occur in soil. This is because soils harbor the greatest concentration of microbes and organic compounds that promote weathering, and because soils have high porosity and more rapid through-flow of water.

A useful metric for chemical weathering potential is the chemical depletion fraction (CDF), which quantifies the overall extent of mineral weathering and mass loss by dissolution (Riebe et al., 2001). In silicate rocks, CDF has been shown to vary systematically with precipitation (P) and temperature (T) across a wide range of climates (White and Blum, 1995; Riebe et al., 2004; West et al., 2005), as

$$CDF = a\left(\frac{P}{P_{ref}}\right)^{b} e^{-\frac{E_a}{R}\left(\frac{1}{T}-\frac{1}{T_{ref}}\right)} \tag{9}$$

where E_a is a representative activation energy, R is the universal ideal gas constant, b is a fit exponent and a is the value of CDF when P and T are equal to reference values (P_{ref}, P_{ref}) near the center of the range of potential values. This relationship was established with data from sites where the weathering rate was primarily limited by the supply of fresh mineral surfaces, not by the residence time available for reactions to reach equilibrium. Whether particles are subject to supply-limited or kinetic-limited weathering depends on the rate constants for specific mineral dissolution reactions (Ferrier et al., 2010), and the rate of physical weathering by erosion, which is ultimately driven by the tectonic boundary conditions (Ferrier and Kirchner, 2008; Norton et al., 2014). To the extent that particle size reduction is influenced by chemical weathering in soils, we might use Eq. (9) to link climate conditions to hillslope sediment size.

The rate of particle size reduction by weathering in soils may also depend on the particle size itself. For example, if rock fragments degrade by the growth and shedding of a weathering rind (Yoo and Mudd, 2008), and we represent fragments as spheres with a uniform and steady rind growth rate, then the fractional change in size, D/D_0, is inversely proportional to size

$$\frac{d(D/D_0)}{dt} = -\frac{u_w}{D_0} \tag{10}$$

where u_w is the velocity of the weathering front within the clast. For survival of rock fragments large enough to become bedload in the channel, the implication of Eq. (10) is that chemical weathering could have a much larger impact on the supply of fine gravel than on fragments in the coarse gravel, cobble and larger size classes.

For weathering rinds to be shed by rock fragments in soil, mechanical wear in transport should play a major role. Soils are mixed and transported downslope by physical disturbances that can drive

frictional contacts and collisions between particles, causing wear. We might expect particle wear rate by physical processes to scale with a metric for the vigor of soil transport, such as soil diffusivity. By analogy with abrasion of rock particles in fluvial transport, physical wear of rock fragments in soil might scale with particle size such that the fractional rate of change is constant

$$\frac{d(D/D_0)}{dt} = -\alpha_s \tag{11}$$

where the soil abrasion coefficient α_s would depend on rock durability and the intensity and frequency of soil mixing. Although the potential influence of dynamic fragmentation on soil particle size distributions has been explored theoretically (Perfect, 1997; Bird et al., 2009), specific physical wear mechanisms within soils have not been well documented.

In contrast, much work has focused on fragmentation of coarse particles by physical processes acting at the ground surface. For example, heating by solar insolation and resulting differential volumetric expansion can generate stresses capable of fracturing rock (McFadden et al., 2005; McGrath et al., 2013). This thermal mechanism can produce fresh rock particles from exposed bedrock as well as break apart rock fragments on soil surfaces (Eppes and Griffing, 2010; Eppes et al., 2010). Other physical mechanisms include fracture due to growth of salt crystals (Wells et al., 2008), segregation ice (Matsuoka and Murton, 2008), wildfire (Shakesby and Doerr, 2006), and lightning (Wakasa et al., 2012). Rates of particle breakdown have been documented using trails of fragments shed by exposed boulders (Putkonen et al., 2014) and modeled using rules for the relative sizes of parent and daughter particles (Sharmeen and Willgoose, 2006; Cohen et al., 2009).

4.3. Residence time in the weathering engine

Weathering takes time. For particles passing through the weathering engine on their journey to the channel, the extent of size reduction by chemical and physical weathering processes will depend on the particle residence time in each hillslope weathering environment. The journey to the channel has two main components, vertical exhumation through the fractured rock and saprolite layers, then lateral transport downslope in the soil or on the surface (Fig. 7).

Exhumation can be viewed in two reference frames. In the reference frame of the surface, rock rises from below at the rate that overlying material is eroded. In the reference frame of a parcel of rock, a sequence of weathering fronts descends from above removing mass through dissolution, until the rock is disrupted by physical processes and discrete particles are produced and entrained in the transport system. At steady state, the weathering front velocity will equal the surface erosion rate. Residence time during exhumation then is simply the sum of the thickness of the vertically layered rock weathering zones H_w divided by erosion rate E_r (Eq. (2)).

In the surface transport system, particle residence time also depends on the proximity to the channel. On convex soil-mantled hillslopes, particles exhumed far from the channel will have relatively longer residence times because they have farther to travel and initially move more slowly on less steep slopes. Conversely, particles exhumed near the channel travel with higher initial velocity and have less distance to cover, so will have relatively shorter residence times. For the case of spatially uniform erosion rate and soil depth, the individual travel times (τ) for particles delivered to the channel will have an exponential distribution (Mudd and Furbish, 2006),

$$P(\tau) = \frac{e^{-\tau/R_t}}{R_t} \tag{12}$$

with a mean residence time R_t equal to the ratio of soil thickness to erosion rate, and a variance equal to the square of R_t. Hence, most travel times through the soil will be brief compared to the average, but a smaller fraction of rock particles will be exposed to weathering in the soil for a relatively long time. The exponential distribution of particle residence times means soil weathering will have two distinct effects, reducing particle size overall, and increasing the spread of the size distribution by lengthening the fine tail.

On soil mantled hillslopes where soil production from bedrock is roughly in balance with channel incision rates, soil thickness varies systematically with erosion rate (Heimsath et al., 1997; Larsen et al., 2014). In many landscapes, soil production rate has been shown to decline exponentially with soil thickness H, which we can write as

$$E = E_0 e^{-H/\beta} \tag{13}$$

where E_0 is the erosion rate when soil depth goes to zero, and β is the length scale for the decline in soil production with increasing soil depth. Rearranging for H we obtain

$$H = \beta \ln(E_0/E) \tag{14}$$

and combining Eq. (14) with Eq. (2) gives

$$R_t = \frac{\beta}{E} \ln(E_0/E). \tag{15}$$

Eq. (15) shows that residence time will be inversely proportional to erosion rate for relatively low erosion rates (i.e. $E \ll E_0$), but as erosion rate approaches E_0, soil residence time decreases toward zero at a rate much $>1/E$.

The non-linear dependence of soil thickness and residence time on erosion rate helps explain why erosion rate could strongly influence particle size supplied to channels. Thinner soils will permit deeper and more frequent penetration of underlying rock by surface geomorphic agents such as trees and burrowing animals, detaching larger fragments of less weathered rock. Shorter residence times limit the progress of chemical weathering reactions in the soil, imposing a kinetic limitation on how much of the climatic and mineralogic potential for chemical weathering is realized. Although more rapid soil transport may mean physical weathering processes are more vigorous, this may be balanced by the fact that rock fragments that are exhumed and transported rapidly are more likely to retain their initial intact rock strength and have higher resistance to physical breakdown.

4.4. Bypassing the soil weathering engine

Even where soils are thin and residence times are short, chemical weathering may still be capable of destroying most coarse particles, in which case soils would supply primarily sand and finer sediments to channels. Thus, in many landscapes, the dominant source of bedload-sized clasts for channels may be coarse rock fragments that bypass the soil weathering engine entirely. There are at least three ways particles can avoid spending time within the soil column. Where soil is present, rocks can bypass it by being lifted directly to the surface from the weathered bedrock beneath the soil, by tree throw or other processes that both produce and mix soils. Rocks can also be exhumed at hillslope locations devoid of soil, such as isolated bedrock outcrops or along bedrock ridges. And rocks can also be produced, transported and delivered to the channel in one brief landslide event. Next we consider each of these three ways of bypassing the soil weathering engine.

The journey through the weathering engine has been described as riding a conveyor belt that moves rock steadily through a natural chemical processing plant (Anderson et al., 2007). Some rocks ride an elevator instead, rising quickly past the intermediate levels of the soil to the relatively safe surface environment. The elevator is often operated by living organisms. For example, tree throw and gopher burrowing can transport rock fragments from the fractured rock below the soil to surface essentially instantaneously. Larger rock fragments may also be

Please cite this article as: Sklar, L.S., et al., The problem of predicting the size distribution of sediment supplied by hillslopes to rivers, Geomorphology (2016), http://dx.doi.org/10.1016/j.geomorph.2016.05.005

preferentially transported vertically by kinetic sieving mechanisms in vigorously mixed soils (Poesen et al., 1997). In many environments, particularly in dry climates, soil surfaces are enriched in rock fragments relative to the soil column (Poesen and Lavee, 1994). Armored soil surfaces may reflect vertical transport to the surface of larger fragments, as well as the effects of sheet wash and other size-selective surface transport processes that winnow finer particles (Issa et al., 2006; Michaelides and Martin, 2012). In general, we might expect the strength of the elevator mechanism to correlate with the same factors that control weathering potential and residence time in soils. For example, faster eroding hillslopes will have thinner soils, permitting deeper penetration of rock by tree roots and shortening the vertical distance that rocks must traverse to reach the surface. Likewise, the relative contribution of the elevator mechanism to the coarse fraction of sediments supplied to channels will depend on the contrast in weathering potential between the soil surface and interior. Although rock fragments at the soil surface are still subject to physical weathering by heating or freezing, the contrast is probably dominated by the factors that control chemical weathering potential within the soil. One expression of this contrast is the occurrence of Tors, isolated rock outcrops surrounded by soil, which can form in homogenous rock due to feedbacks between wetness and weathering (Heimsath et al., 2000; Strudley et al., 2006).

Tors are just one of many examples of hillslope settings where rock is not mantled by soil. More broadly, the presence or absence of soil can be influenced by all of the independent variables we identified previously, including lithology, climate, life, erosion rate and topography. For example, bare bedrock is found where local lithology severely limits nutrients available for plant growth (Hahm et al., 2014) or does not provide fractures for trees to take root (Marshall and Roering, 2014). Bedrock hillslopes dominate in many arid or cold climates because chemical weathering and biotic activity are so limited that soils cannot form or persist (Amundson et al., 2012; Balco and Shuster, 2009). And where rates of rock uplift and erosion are very rapid, hillslopes are often poised at a steep threshold gradient where bedrock landsliding dominates (Clarke and Burbank, 2010).

Erosion rate provides an independent variable that could be used to parameterize the threshold between soil-mantled and bedrock hillslopes. Where rates of base level lowering exceed E_0, the maximum erosion rate in the exponential soil production function (Eq. (13)), soil does not accumulate and slopes are stripped of soil. Even where thin soils are present, soil cover can be patchy. One possible explanation for patchy soil cover is a feedback between erosion rate and the maximum possible rate of soil production, due to enhanced chemical weathering and an increase in the frequency of shallow landslides (Dixon et al., 2012; Heimsath et al., 2012). Other examples include where rock joint spacing is wide and large blocks are exhumed to the surface (Riggins et al., 2011) and where erosion rates vary significantly at the scale of individual hillslopes (Larsen et al., 2014). Available data suggest that the soil-bedrock transition corresponds with maximum soil production rates E_0 across a wide range of 0.03 to 3.0 mm/yr (Larsen et al., 2014; Milodowski et al., 2015), although the broader influence of lithology, climate and biota on E_0 remains poorly understood.

The same factors that favor bare bedrock hillslopes, such as rapid erosion rates and cold or arid climates, are also likely to limit the extent of chemical weathering and the residence time of rock as it passes through the lower critical zone. Hence we expect bedrock hillslopes to be dominated by physical, rather than chemical weathering processes. On steep bedrock slopes, gravitational stresses and co-seismic ground accelerations initiate and propagate fractures that produce mobile rock particles across the full range of possible sizes. Rock fall from near-vertical cliffs produces some of the largest boulders (e.g. Zimmer et al., 2012), but also a wide size distribution from shattering of rock fragments on impact (Wieczorek et al., 2000). Rock avalanches begin as large mass failures but generate wide particle size distributions through comminution in transport, a process that helps to prolong motion of the granular mass (Davies et al., 1999). Particle size distributions of rock avalanche and landslide debris (Casagli et al., 2003; Attal and Lavé, 2006; Whittaker et al., 2010) may provide insight into the original size distribution of rock fragments, if the extent of breakdown in transport can be determined. In general, we expect bedrock landslides to deliver the coarsest size distributions that channels receive, and where erosion rates are highest to most closely reflect the original distribution of fracture spacing in the unweathered bedrock.

4.5. Where in a catchment do coarse sediments originate?

Variation in weathering intensity and residence time on the many possible pathways taken by particles moving down hillslopes should lead to patterns in the spatial distribution of source areas for coarse material reaching the channel. Several possible scenarios are depicted in Fig. 9 for an idealized first-order catchment. The simplest pattern is a uniform distribution (Fig. 9A), which is what is implicitly assumed in current landscape evolution models that include the effects of bedload sediment. However, where weathering potential is high and mean residence time is long, coarse sediment may be sourced primarily at the base of the hillslope, adjacent to the channel (Fig. 9B), because coarse particles exhumed farther upslope are reduced to sand and finer sizes before reaching the channel. The opposite pattern (Fig. 9C) might occur where soils are thin or absent along the ridges but are thicker downslope (as depicted in Fig. 7). In this case, coarse sediment may only be produced along the ridges, and the bedload supply is composed of those particles that survived the downslope journey by staying on the soil surface. Where bedrock outcrops are more randomly distributed, for example due to small scale variations in underlying lithology, isolated coarse sediment sources may be scattered across the catchment (Fig. 9D). Another pattern might arise where weathering conditions differ dramatically with hillslope aspect (Fig. 9E). In this case, coarse sediment might be primarily sourced on only one side of a catchment, for example where chemical weathering is more intense on cooler north-facing slopes that retain water longer than warmer south-facing slopes (Fig. 6). Many other patterns are possible as well, such as a downslope gradient in the relative contribution of coarse sediment, due to differences in local climate or erosion rate with elevation (Fig. 9F). These examples suggest that observations of such patterns in the field could be diagnostic of weathering conditions, useful for estimating size and abundance of coarse sediment supply, and helpful in predicting how sediment supply might be affected by changes in landuse or climate.

5. A modeling framework

We next consider how to use the potential input variables and functional relationships described above in a simple predictive model for the size distribution of sediments supplied by hillslopes to channels. Our goal is to explore a general modeling framework, which could be adapted for specific landscape settings or further developed with better understanding of the mechanisms of hillslope sediment production and weathering. Ultimately, the modeling framework developed below is an exploration of the hypothesis that landscape-scale trends in the size of sediment supplied to channels exist, and can be quantified with knowledge of a few key independent variables.

We begin by defining the model in terms of a weathering function W that transforms an initial size distribution $P(D_0)$ of particles produced from bedrock into the size distribution $P(D_c)$ of particles delivered to the channel, i.e.

$$P(D_c) = f(W, P(D_0)) \tag{16}$$

where W depends on the climatic and geomorphic factors that control the style and intensity of weathering. The initial size distribution could be specified with an exponential (Eq. (6)) or fractal (Eq. (8)) distribution, with the parameter values chosen to reflect intact rock strength, joint spacing, or a size-selective sediment production process.

Please cite this article as: Sklar, L.S., et al., The problem of predicting the size distribution of sediment supplied by hillslopes to rivers, Geomorphology (2016), http://dx.doi.org/10.1016/j.geomorph.2016.05.005

Given that particle sizes on hillslopes and in channels vary over many orders of magnitude, the simplest transformation would use W as an exponent in a power function

$$D_C = D_{\min}^{W} D_0^{(1-W)} \quad (0 \le W \le 1) \tag{17}$$

where the value of W is constrained to be between 0 (i.e. no weathering, $D_C = D_0$) and 1.0 (complete weathering, $D_C = D_{min}$ for all D_0), and D_{min} is the smallest relevant particle size (e.g. particles <1 μm might be considered part of the dissolved load). The limiting case of W = 0 plots as a 1:1 line on a log-log graph of D_0 vs. D_C (Fig. 10). Graphically, values of W ($1 > W > 0$) in Eq. (17) can be interpreted as a line through which the initial probability density function plotted along the D_0 axis is reflected onto the D_C axis, shifting the mass fraction in each size of the distribution to lower values. This graphical approach is not limited to log-log linear transformations. For example, W could also be a function of grain size, which would create a non-linear transformation that could also be plotted in the functional space depicted in Fig. 10.

For simplicity, we start with the assumption that the magnitude of W captures only the effects of chemical weathering on the hillslope, and that physical weathering processes act primarily to produce the initial size distribution rather than modify it during hillslope transport. We further assume that particle size reduction due to weathering scales with extent of weathering of soluble minerals, as represented by the chemical depletion fraction (*CDF*). For the case when erosion rate is low, residence time is long, and chemical weathering is supply-limited, we can express W as the product of the fraction of soluble minerals (F_{SM}) and a function representing the chemical weathering potential (*CWP*) of the hillslope environment

$$W_{SL} = F_{SM} \cdot CWP \tag{18}$$

where the subscript '*SL*' indicates supply limited conditions. We use the *CDF* framework of Riebe et al. (2004) to express *CWP* as a modified form of Eq. (9)

$$CWP = \left(\frac{P}{P_{\max}}\right)^{b} e^{-\frac{E_a}{R}\left(\frac{1}{T}-\frac{1}{T_{\max}}\right)} \tag{19}$$

where P_{max} and T_{max} represent the combination of P and T conditions where weathering potential is maximized. Hence, when $P = P_{max}$ and $T = T_{max}$, $CWP = 1$ and $W_{SL} = F_{SM}$, i.e. all soluble minerals are completely weathered and the residual material is composed only of insoluble minerals. In all other cases, precipitation and temperature are constrained to be less than the maximum (i.e. $0 < P < P_{max}$; $T_{min} < T < T_{max}$) and the range of W is $0 \le W_{SL} < F_{SM}$. Fig. 11 shows contours of *CWP* in P, T space as calculated with Eq. (19).

When erosion rate exceeds a threshold value, chemical weathering is no longer limited by the supply of fresh minerals, but instead becomes limited by the residence time available for weathering reactions to progress to completion. We define an erosion rate E_{SK}, as determining the transition between supply- and kinetic-limited weathering. For erosion rates greater than E_{SK}, the value of W will be less than W_{SL} due to the kinetic limitation. As erosion rate increases even further, a second threshold is reached, where erosion is so rapid that negligible weathering occurs, and fresh unweathered rock is exhumed and eroded into the channel without any significant effect of the weathering engine. To represent this transition, we define a second threshold erosion rate E_{KU}. As erosion rate increases toward E_{KU}, W should approach zero, to represent negligible transformation of the initial size distribution for negligible residence time in the hillslope surface environment. The two threshold erosion rates, E_{SK} and E_{KU}, which bound the range of kinetic-limited weathering, can be used to define a complete functional

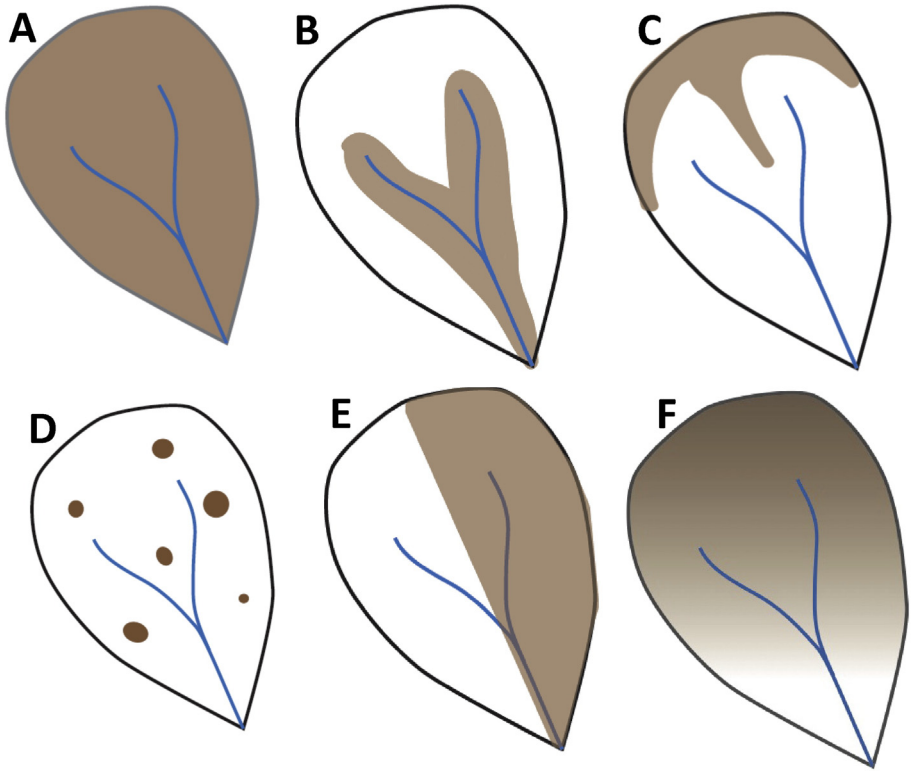

Fig. 9. Scenarios for spatial variation in production of coarse sediment supplied to channels, in an idealized upland catchment. (A) Uniform: course sediment sourced equally across catchment. (B) Near-channel: only rock fragments with shortest travel distances survive weathering engine to enter channel as bedload-sized clasts. (C) Ridge-line: thin or absent soils along ridges permit rock fragments to bypass intense weathering that occurs in soils downslope; coarse particles reaching channel travel on surface. (D) Isolated: only bedrock outcrops or small landslides provide coarse sediments. (E) Aspect-controlled: large cross-valley contrasts in solar insolation may affect controls on weathering potential such as moisture retention, vegetation, and topographic slope. (F) Gradient: weathering conditions may shift continuously from ridge to outlet, such that coarse sediments a produced everywhere but in greater abundance closer to the ridges.

Please cite this article as: Sklar, L.S., et al., The problem of predicting the size distribution of sediment supplied by hillslopes to rivers, Geomorphology (2016), http://dx.doi.org/10.1016/j.geomorph.2016.05.005

form for the variation in W with erosion rate E over the range $E_{SK} \le E \le E_{KU}$

$$W = W_{SL}\left[1-\left(\frac{E-E_{SK}}{E_{KU}-E_{SK}}\right)^{\varphi}\right] \quad (20)$$

where the exponent φ is set to 2/3 to capture the non-linear dependence of residence time on erosion rate discussed above (Eq. (15)). If $E < E_{SK}$ then $W = W_{SL}$ and when $E > E_{KU}$ then $W = 0$. Combining Eqs. (18), (19) and (20), we can write the full particle size transformation function as

$$W = F_{SM}\left(\frac{P}{P_{\max}}\right)^{b} e^{-\frac{E_a}{R}\left(\frac{1}{T}-\frac{1}{T_{\max}}\right)}\left[1-\left(\frac{E-E_{SK}}{E_{KU}-E_{SK}}\right)^{\varphi}\right]. \quad (21)$$

Here we set $b = 0.5$ and $E_a = 60$ kJ/mol based on an analysis of chemical depletion in granitic terrain (Riebe et al., 2004; West et al., 2005). Eq. (21) is plotted in Fig. 12, for various values of F_{SM}, with P and T set to maximum values.

To illustrate how this modeling framework can be used to predict the effects of climate or erosion rate on sediment size distributions supplied to channels, we consider several weathering scenarios. In each scenario we represent the initial size distribution of particles produced from bedrock with exponential distributions taken from the example curves in Fig. 8a. First, consider a pattern of climatic variation in mean annual precipitation and temperature that causes chemical weathering potential (*CWP*) to vary from very low (0) to very high 1.0. Assuming that 60% of the rock is composed of soluble minerals ($F_{SM} = 0.6$), and that erosion rates are low enough that weathering is supply-limited ($E < E_{SK}$), then the corresponding values of the weathering function W will range between 0 and 0.6. Fig. 13 shows how a relatively coarse input size distribution ($k = 100$ mm, $n = 0.95$) is transformed into progressively finer and narrower output distributions as *CWP* and W increase from 0. The values of *CWP* and W for each curve in Fig. 13 are indicated by colored squares in Figs. 11 and 12. The same pattern of size reduction by weathering can also be obtained by holding climate constant and varying erosion rate within the kinetically-limited regime ($E_{SK} < E < E_{KU}$). This is shown in Fig. 12 by the colored circles, which indicate the erosion rates that yield the same values of the weathering function W, for the case where $F_{SM} = 0.6$ and $CWP = 1$ (i.e. T and P are at max values).

The next two scenarios illustrate how hillslope weathering could transform a uni-modal initial size distribution into a bimodal distribution of sediments supplied to channels. In the first case, we assume that only a fraction of the exhumed sediment is subjected to a relatively strong weathering environment while the rest experiences weaker weathering. This could arise where soil only covers part of the hillslope (Fig. 9C) or where aspect strongly influences weathering (Fig. 9E). If we use $CWP = 0.8$ and 0.2 for the strong and weak weathering respectively, the initial size distribution ($k = 30$; $n = 0.60$) is transformed into two size distributions, one coarse, the other much finer. When these two distributions are added together they produce a bimodal composite distribution as shown in Fig. 14A.

Another way bimodal distributions could be produced is if the weathering function W depends on particle size. If we conceptualize particle size reduction as the growth and shedding of a weathering rind (Eq. (10)), we can express the thickness of the weathering rind as the product of the velocity of the weathering front within the clast u_w and the residence time R_t. The rind thickness should be proportional to W (Eq. (21)), because the value of W depends on the climatic and mineralogic factors that control u_w and on erosion rate which controls residence time

$$u_w R_t \propto W \quad (22)$$

The relative effect of rind removal on particle size scales inversely with initial size, so we define a size dependent exponent W_D as

$$W_D = \frac{\lambda W}{D_0} \quad (23)$$

where the constant λ represents the particle size that will be completely weathered (i.e. the weathering rind is equal to the particle radius). Then, for $\lambda/D_0 < 1$ (incomplete weathering) we use W_D as the exponent in the size transformation expression (Eq. (17))

$$D_c = D_{\min}^{W_D} D_0^{1-W_D} \quad (24)$$

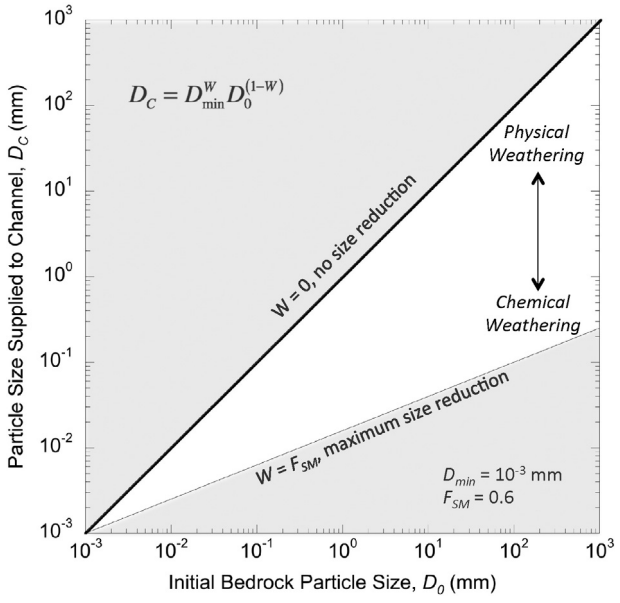

Fig. 10. Modeling framework definition sketch. Within this model space, input particle size distributions $P(D_0)$ can be transformed to the size distribution supplied to the channel $P(D_c)$ by a weathering function (distributions not shown). Here the transformation function is a power equation (Eq. (17)), which plots as a straight line in log-log space. When no chemical weathering occurs, the exponent $W = 0$, there is no change in the size ($D_0 = D_c$), and the slope of the line is unity. When chemical weathering potential is maximized ($CWP = 1$), the value of W is equal to the fraction of soluble minerals (F_{SM}, here set to 0.6 for illustration), and the slope of the line is $1 - F_{SM}$. These two lines provide upper and lower bounds to the range of possible size changes. Within these bounds (unshaded domain), the dominant weathering mode shifts from physical to chemical as the value of W increases from 0 to F_{SM}. The model parameter D_{min} represents the smallest relevant particle size, and serves as an intercept for the transformation function.

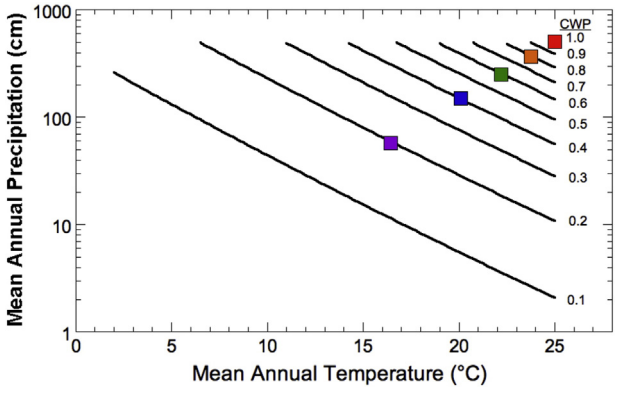

Fig. 11. Contours of chemical weathering potential (*CWP*) as function of mean annual temperature (T) and precipitation (P) (Eq. (19)). When T and P are at maximum values, $CWP = 1$. Colored squares correspond to variation in CWP shown in Fig. 12. Here activation energy $E_a = 60$ kJ/mol, $T_{max} = 25$ °C, and $P_{max} = 500$ cm/yr. (For interpretation of the references to color in this figure legend, the reader is referred to the web version of this article.)

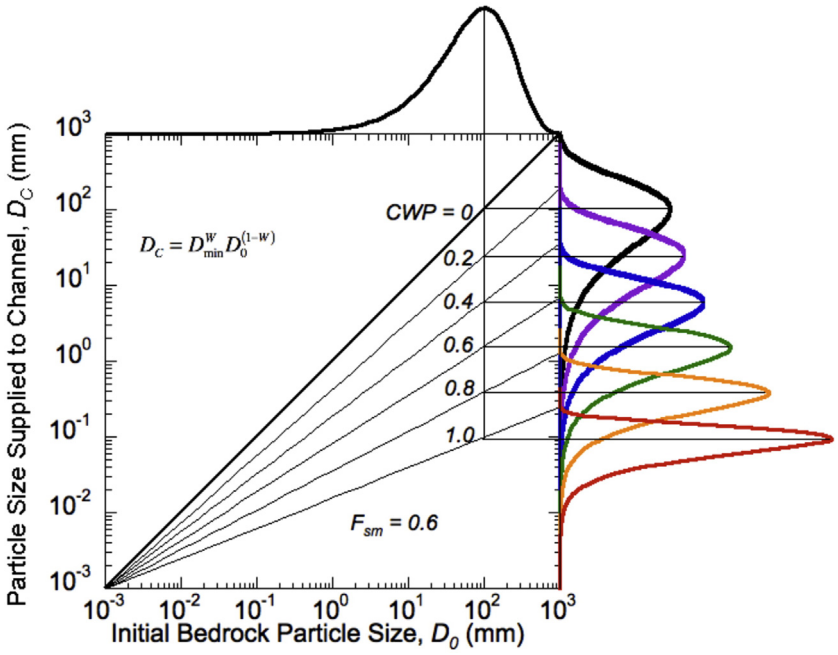

Fig. 13. Modeled particle size transformations across range of chemical weathering potential (*CWP*). Initial size distribution, by mass, ($P(D_0)$, black curve plotted along upper horizontal axis) assumed to be exponential (Eq. (6)), with $k = 100$ and $n = 0.95$ (Fig. 8A). Colored curves plotted along right vertical axis show transformed size distributions $P(D_C)$ for values of *CWP* ranging from 0 (no weathering) to 1.0 (maximum weathering), for fraction of soluble minerals $F_{SM} = 0.6$. Thin black lines show transformation of distribution mode. Note decrease in width of transformed distributions with greater weathering. (For interpretation of the references to color in this figure legend, the reader is referred to the web version of this article.)

while for $\lambda/D_0 \geq 1$ the exponent W has the value F_{SM} to be consistent with the assumption of complete weathering. This is illustrated in Fig. 14B, where the transformation function has a constant slope for $D_0 < \lambda$ (where $\lambda = 1$ mm), but becomes non-linear for $D_0 > \lambda$, and asymptotes to the unweathered line for largest initial sizes. For a relatively wide input size distribution ($k = 10$; $n = 0.45$) a bimodal output distribution results. The gap between the two modes in the output size distribution occurs where the transformation function is strongly non-linear. For the parameter values chosen in this example, this model outcome represents a hillslope weathering environment where fine gravel and coarse sand weather into finer sand and silt particles, while the sizes of larger rock fragments are relatively unaltered by weathering.

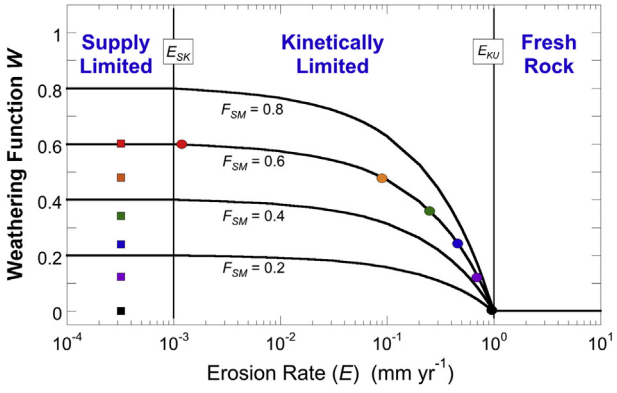

Fig. 12. Modeled influence of erosion rate on weathering regime. For low erosion rates, weathering is limited by the supply of fresh mineral surfaces and depends only on chemical weathering potential (*CWP*) and fraction of soluble minerals (F_{SM}) (Eqs. (18) and (19)) At intermediate erosion rates, weathering is limited by the residence time available for kinetic reactions to proceed to completion; E_{SK} represents the threshold between supply- and kinetically-limited weathering. For erosion rates greater than a second threshold value (E_{KU}), residence time is negligible and fresh rock is supplied to the channel. (Magnitudes of E_{SK} and E_{KU} for illustration only). In the kinetically-limited regime, variation in weathering exponent W is given by Eq. (21). Colored symbols illustrate how similar values of W can occur either due to variation in chemical weathering potential (circles) or erosion rate (squares). (For interpretation of the references to color in this figure legend, the reader is referred to the web version of this article.)

6. Discussion

6.1. Connecting hillslopes to channels

Our analysis and model framework provides theoretical support for the hypothesis that downstream changes in fluvial sediment size distributions may often be driven by changes in hillslope sediment supply. The independent factors we considered, lithology, climate, biota and erosion rate, are rarely spatially uniform, and commonly have systematic gradients at the catchment scale. For example, in mixed lithologies with large differences in strength, elevated ridges are more likely to be composed of stronger rocks, while weaker rocks commonly underlie lower elevation valley bottoms. In such settings we might expect more widely spaced joints in the stronger rock and thus coarser sediment supply from higher elevations. Similarly, the typical variation in mean annual temperature with elevation follows the adiabatic lapse rate of ~6 °C km^{-1}. For 1 km of relief, this can change chemical weathering potential by a factor of 2 (Eq. (19), Fig. 11), producing coarser sediment at higher, colder elevations within a catchment. Weathering potential can also vary with elevation due to orographic gradients in precipitation, and shifts in ecosystem processes. We might also expect hillslope sediment size to vary where erosion rate varies between catchment headwaters to outlet, for example where accelerated base-level lowering drives upstream knickpoint migration and hillslope steepening (Gallen et al., 2011; Hurst et al., 2012), or where the highest topography coincides with the most rapid uplift rates and frequent landslides (Montgomery and Brandon, 2002). The evidence from Inyo Creek is consistent with these hypotheses. There, hillslope sediment size, as gleaned from geochemical tracers (Fig. 1A) and field point counts (Fig. 5), is larger at higher elevations, which are colder, less-vegetated, steeper and more rapidly eroding (Riebe et al., 2015).

We also find support for the hypothesis that bimodality in river sediment distributions has its origins in hillslope weathering. At least four distinct sets of mechanisms could produce bimodal supply to rivers.

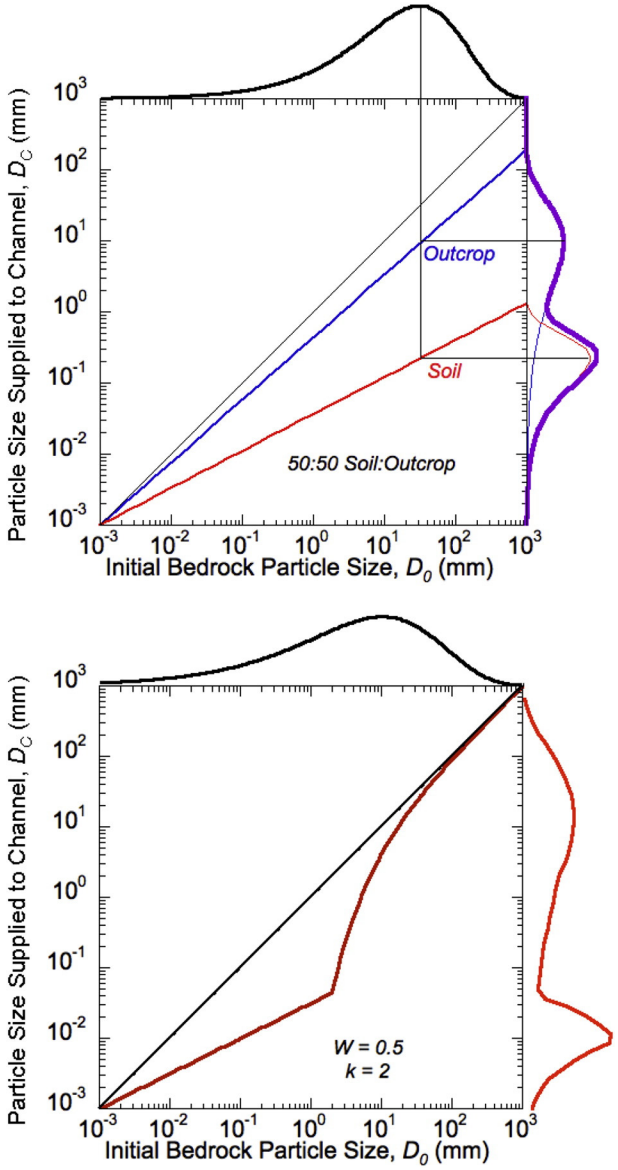

Fig. 14. Two scenarios for creation of bimodal particle size distributions by hillslope weathering. (A) Rock exhumation divided between soil-mantled locations and bare bedrock outcrops (as in Fig. 9, panels C, D or E), with differing chemical weathering potential, assuming $CWP = 0.2$ for outcrop and $CWP = 0.8$ for soil, and 50:50 partitioning. Input size distribution (black curve, top horizontal axis) assumed exponential (Eq. (6)), with $k = 30$ and $n = 0.6$ (Fig. 8A). Size distribution supplied to channels (purple curve, right vertical axis) is sum of two uni-modal distributions produced by outcrops (blue) and soil (red). (B) Size-dependent particle weathering in soil (Eqs. (23), (24)) for particles larger than 2 mm ($\lambda = 2$), with weathering exponent $W = 0.5$ for particles smaller than 2 mm. Input size distribution assumed exponential, with $k = 10$ and $n = 0.45$. (For interpretation of the references to color in this figure legend, the reader is referred to the web version of this article.)

The first case is where large differences in weathering potential occur at the hillslope scale (Fig. 14A), such as between bedrock outcrops and adjacent soil-mantled areas, north- and south-facing slopes (e.g. Fig. 6), or where a significant fraction of exhumed rock particles bypass the soil weathering engine via tree-throw and other 'elevator' mechanisms. A second case is where grain size reduction in soils is size-dependent, such that particles in the middle of the source size distribution are most susceptible to size reduction by chemical weathering (Fig. 14B). The third case arises when lithology, climate, and tectonics favor weathering processes that produce both gruss and boulders, such as in biotite-rich granitic rocks in relatively dry, slow-eroding landscapes (Fig. 3C). Finally, bimodal size distributions characterize sediments delivered to channels by landslides (Casagli et al., 2003; Attal and Lavé, 2006), possibly due to a tendency for larger rocks to preferentially crush moderate-sized particles in granular flows (Caballero et al., 2014).

6.2. Model framework

The examples shown in Figs. 13 and 14 illustrate how our modeling framework can be used to represent particle size production and weathering in a wide variety of hillslope settings. This level of generality was one of our goals in crafting a model that, in the spirit of the 'geomorphic transport law' (Dietrich et al., 2003), balances mechanistic realism with computational simplicity, such that it could be applied in a landscape evolution model. An important element of our model development is distinguishing between the initial size distribution of the unweathered rock, and its transformation by weathering on the journey from the point of exhumation to the channel. A key question for further investigation is which of these two model components dominates the size distribution supplied to real channels? For example, at the limited scale of a single mapped lithologic unit, are spatial variations in the size supplied to channels dominated by variation in local weathering processes (Attal et al., 2015), while at larger scales, do the effects of differing lithology dominate (Miller, 1958)? In our model framework, we might expect the answer to lie in the relative contributions of physical and chemical weathering processes. In cold, steep, rapidly eroding landscapes, where physical processes dominate, we might expect the initial size distribution to arrive in the channel with little alteration. Conversely, in landscapes with warmer temperatures and longer hillslope residence times, any effect of variations in the initial distribution may be overwhelmed by the profound transformation of particle size by chemical weathering.

To better explore the tradeoffs between physical and chemical weathering processes, the model framework might be expanded to explicitly include physical mechanisms for particle size reduction. If particle breakdown in hillslope transport is analogous to size reduction in fluvial abrasion (Eq. (11)), then the model as presented above can already be used. In that case, the value of transformation function W would depend on the abrasion coefficient (α_s) and a parameterization of residence time

$$W \propto \alpha_s R_t \tag{25}$$

W would have a constant value for all input sizes above a minimum size, below which particle contact forces are too small or infrequent to cause wear. Other physical processes might require an explicit parameterization if they preferentially produce transportable fragments in a certain size range. For example, if frost cracking selectively produces cobble-sized talus, then the transformation function W might have an additional temperature term, which at sufficiently cold temperatures would have a non-linearity that focuses transformed sizes into the cobble-size range. More broadly, the relative importance of physical weathering mechanisms should scale with hillslope gradient, a fundamental geomorphic variable that we chose not to include in this initial model exploration. One way to include slope would be to use it in place of erosion rate, because hillslope transport rate and thus residence time varies with slope (Almond et al., 2007). In this case, W should go to zero as slope approaches a threshold value where erosion is dominated by bedrock landslides (Ouimet et al., 2009). Similarly, as slope declines and residence time grows long, chemical weathering should shift to supply-limited, and physical processes should have little influence.

To more explicitly account for the influence of topography and geomorphic process regime, an alternative modeling framework might predict size distribution from mechanisms of sediment delivery to channels. This could be built on field measurements of distributions delivered by common geomorphic processes, such as sheetwash, creep, dry ravel, shallow landsliding, deep-seated earth flows, and bedrock landslides. The relative contribution of each process could be

estimated from the spatial distribution of topographic attributes associated with each process domain. This empirical framework would be less appropriate for building a mechanistic understanding of the controls on particle size production and evolution on hillslopes, and would require more explicit representation of fine-scale hillslope topography. However, the data needed to parameterize such a model will be needed in any case for testing and refining more theoretical models such as the framework presented here. Another channel-centered, empirical approach could make use of existing and new data on channel bed material and bedload and suspended sediment flux. For example, size distributions of sediments moving through low-order channels should largely reflect the integrated contributions of adjacent hillslopes, enabling hypothesis tests that compare multiple headwater catchments across gradients in lithology, climate or erosion rate. Similarly, downstream sequences of size-specific sediment flux measurements can be compared to changes in the attributes of hillslopes in the accumulated drainage area, to test for the influence of hillslope supply (Struck et al., 2015).

A key challenge in developing empirical models and testing theoretical models will be measuring representative particle size distributions across the vast range of geomorphic, lithologic and climate settings that a general model might be applied to. For the model framework presented here, measurements of the latent size distributions in unweathered bedrock are also needed. Recent studies have advanced new techniques for characterizing size distributions in rocky soils and landslide deposits (Casagli et al., 2003; Attal and Lavé, 2006; Tetegan et al., 2012; Attal et al., 2015), however in some settings the number and volume of samples needed may be very large because of high spatial variability and a wide range of particle sizes. Mining of existing soils data bases (e.g. Marshall and Sklar, 2012) is an efficient and largely untapped alternative, although too often in soils studies the sizes of rock fragments larger than 2 mm are not recorded, and sample volumes are too small to reliably detect larger particles. A promising new approach is to use thermochronometric tracers such as apatite-helium age combined with cosmogenic isotopes, stratified by size class (Riebe et al., 2015; Lukens et al., 2015), to infer the size distribution produced at source locations. Other new approaches are needed to characterize sub-surface particle size and fracture spacing distributions, for example using ground penetrating radar and other geophysical imaging techniques (Neal, 2004; Parsekian et al., 2015). Ultimately, obtaining the data needed to develop and test predictive models of particle size production on hillslopes and delivery to channels will require leveraging existing field research infrastructure such as the network of Critical Zone Observatories and experimental catchments worldwide (Brantley et al., 2007).

7. Conclusion

In conclusion, we find both theoretical and empirical support for the hypothesis that the size distribution of sediments supplied by hillslopes to channels varies in predictable patterns across landscapes. Although the available data are limited, previously published data along with new measurements presented here reveal systematic variations in hillslope particle size with lithology, climate, topography and erosion rate. We demonstrate how these landscape-scale independent variables can be incorporated in a simple modeling framework, which encompasses two primary controls. The first is the latent distribution of spacing between fractures that sets the initial size distribution of particles supplied to the surface by rock exhumation. The second is the transformation of particle size by weathering processes in the critical zone. Consideration of the many possible paths particles can take through the surface weathering zone highlights the large diversity of physical and chemical mechanisms at work, and the rich portfolio of research questions that need to be answered to solve the overarching problem of predicting the sediment size distribution supplied to channels. Solving this problem is necessary to understand how hillslopes influence sediment size variation through river networks, and ultimately to understand the feedbacks between hillslope weathering and river incision that govern landscape evolution.

Acknowledgments

For assistance in field data collection we thank Nick Aeilo, Omid Arabnia, Gionata Bianchi, Skye Corbett, Theresa Fritz-Endres, Brian Fuller, Jason Guldman, Molly Mclaughlin, Peter Polito, Sam Shaw, and Joey Verdian. We also thank Ron Amundson, Bill Dietrich, and Ken Ferrier for thoughtful discussions, and Mikael Attal for helpful review comments. Funding is provided by NSF grants EAR 1324830 to LSS and EAR 1239521 to CSR, and the Doris and David Dawdy Fund for Hydrologic Science at SFSU.

References

Almond, P., Roering, J., Hales, T.C., 2007. Using soil residence time to delineate spatial and temporal patterns of transient landscape response. J. Geophys. Res. Earth Surf. 112 (F3).
Attal, M., Lavé, J., 2006. Changes of bedload characteristics along the Marsyandi River (central Nepal): implications for understanding hillslope sediment supply, sediment load evolution along fluvial networks, and denudation in active orogenic belts. Geol. Soc. Am. Spec. Pap. 398, 143–171.
Attal, M., Mudd, S.M., Hurst, M.D., Weinman, B., Yoo, K., Naylor, M., 2015. Impact of change in erosion rate and landscape steepness on hillslope and fluvial sediments grain size in the Feather River Basin (Sierra Nevada, California). Earth Surf. Dyn. 3 (1), 201.
Amundson, R., Dietrich, W., Bellugi, D., Ewing, S., Nishiizumi, K., Chong, G., Caffee, M., 2012. Geomorphologic evidence for the late Pliocene onset of hyperaridity in the Atacama Desert. Geol. Soc. Am. Bull. 124 (7–8), 1048–1070.
Amundson, R., Heimsath, A., Owen, J., Yoo, K., Dietrich, W.E., 2015. Hillslope soils and vegetation. Geomorphology 234, 122–132.
Anderson, S.P., von Blanckenburg, F., White, A.F., 2007. Physical and chemical controls on the critical zone. Elements 3 (5), 315–319.
Anderson, R.S., Anderson, S.P., Tucker, G.E., 2013. Rock damage and regolith transport by frost: an example of climate modulation of the geomorphology of the critical zone. Earth Surf. Process. Landf. 38 (3), 299–316.
Balco, G., Shuster, D.L., 2009. Production rate of cosmogenic 21 Ne in quartz estimated from 10 Be, 26 Al, and 21 Ne concentrations in slowly eroding Antarctic bedrock surfaces. Earth Planet. Sci. Lett. 281 (1), 48–58.
Bird, N.R.A., Watts, C.W., Tarquis, A.M., Whitmore, A.P., 2009. Modeling dynamic fragmentation of soil. Vadose Zone J. 8 (1), 197–201.
Bittelli, M., Campbell, G.S., Flury, M., 1999. Characterization of particle-size distribution in soils with a fragmentation model. Soil Sci. Soc. Am. J. 63 (4), 782–788.
Blenkinsop, T.G., 1991. Cataclasis and processes of particle size reduction. Pure and. Appl. Geophys. 136 (1), 59–86.
Booth, A.M., Roering, J.J., Rempel, A.W., 2013. Topographic signatures and a general transport law for deep-seated landslides in a landscape evolution model. J. Geophys. Res. Earth Surf. 118 (2), 603–624.
Brantley, S.L., Lebedeva, M., 2011. Learning to read the chemistry of regolith to understand the critical zone. Annu. Rev. Earth Planet. Sci. 39, 387–416.
Brantley, S.L., Goldhaber, M.B., Ragnarsdottir, K.V., 2007. Crossing disciplines and scales to understand the critical zone. Elements 3 (5), 307–314.
Caballero, L., Sarocchi, D., Soto, E., Borselli, L., 2014. Rheological changes induced by clast fragmentation in debris flows. J. Geophys. Res. Earth Surf. 119 (9), 1800–1817.
Cai, M., 2011. Rock mass characterization and rock property variability considerations for tunnel and cavern design. Rock Mech. Rock. Eng. 44, 379–399. http://dx.doi.org/10.1007/s00603-011-0138-5.
Casagli, N., Ermini, L., Rosati, G., 2003. Determining grain size distribution of the material composing landslide dams in the Northern Apennines: sampling and processing methods. Eng. Geol. 69 (1), 83–97.
Chadwick, O.A., Gavenda, R.T., Kelly, E.F., Ziegler, K., Olson, C.G., Elliott, W.C., Hendricks, D.M., 2003. The impact of climate on the biogeochemical functioning of volcanic soils. Chem. Geol. 202 (3), 195–223.
Church, M., 2006. Bed material transport and the morphology of alluvial river channels. Annu. Rev. Earth Planet. Sci. 34, 325–354.
Clair, J.S., Moon, S., Holbrook, W.S., Perron, J.T., Riebe, C.S., Martel, S.J., Carr, B., Harman, C., Singha, K., 2015. Geophysical imaging reveals topographic stress control of bedrock weathering. Science 350 (6260), 534–538.
Clarke, B.A., Burbank, D.W., 2010. Bedrock fracturing, threshold hillslopes, and limits to the magnitude of bedrock landslides. Earth Planet. Sci. Lett. 297 (3), 577–586.
Cook, K.L., Turowski, J.M., Hovius, N., 2013. A demonstration of the importance of bedload transport for fluvial bedrock erosion and knickpoint propagation. Earth Surf. Process. Landf. 38 (7), 683–695.
Cohen, S., Willgoose, G., Hancock, G., 2009. The mARM spatially distributed soil evolution model: a computationally efficient modeling framework and analysis of hillslope soil surface organization. J. Geophys. Res. Earth Surf. 114 (F3).
Cowie, P.A., Whittaker, A.C., Attal, M., Roberts, G., Tucker, G.E., Ganas, A., 2008. New constraints on sediment-flux–dependent river incision: Implications for extracting tectonic signals from river profiles. Geology 36 (7), 535–538.
Davies, T.R., McSaveney, M.J., Hodgson, K.A., 1999. A fragmentation-spreading model for long-runout rock avalanches. Can. Geotech. J. 36 (6), 1096–1110.

Please cite this article as: Sklar, L.S., et al., The problem of predicting the size distribution of sediment supplied by hillslopes to rivers, Geomorphology (2016), http://dx.doi.org/10.1016/j.geomorph.2016.05.005

Dietrich, W.E., Perron, J.T., 2006. The search for a topographic signature of life. Nature 439 (7075), 411–418.
Dietrich, W.E., Bellugi, D.G., Sklar, L.S., Stock, J.D., Heimsath, A.M., Roering, J.J., 2003. Geomorphic transport laws for predicting landscape form and dynamics. Prediction Geomorphology 103–132.
Dixon, J.L., Hartshorn, A.S., Heimsath, A.M., DiBiase, R.A., Whipple, K.X., 2012. Chemical weathering response to tectonic forcing: a soils perspective from the San Gabriel Mountains, California. Earth Planet. Sci. Lett. 323, 40–49.
Doyle, M.W., Shields, F.D., 2000. Incorporation of bed texture into a channel evolution model. Geomorphology 34 (3), 291–309.
Egholm, D.L., Knudsen, M.F., Sandiford, M., 2013. Lifespan of mountain ranges scaled by feedbacks between landsliding and erosion by rivers. Nature 498 (7455), 475–478.
Eppes, M.C., Griffing, D., 2010. Granular disintegration of marble in nature: a thermal-mechanical origin for a grus and corestone landscape. Geomorphology 117 (1), 170–180.
Eppes, M.C., McFadden, L.D., Wegmann, K.W., Scuderi, L.A., 2010. Cracks in desert pavement rocks: further insights into mechanical weathering by directional insolation. Geomorphology 123 (1), 97–108.
Ferguson, R., Hoey, T., Wathen, S., Werritty, A., 1996. Field evidence for rapid downstream fining of river gravels through selective transport. Geology 24 (2), 179–182.
Ferrier, K.L., Kirchner, J.W., 2008. Effects of physical erosion on chemical denudation rates: a numerical modeling study of soil-mantled hillslopes. Earth Planet. Sci. Lett. 272 (3), 591–599.
Ferrier, K.L., Kirchner, J.W., Riebe, C.S., Finkel, R.C., 2010. Mineral-specific chemical weathering rates over millennial timescales: measurements at Rio Icacos, Puerto Rico. Chem. Geol. 277 (1), 101–114.
Finnegan, N.J., Sklar, L.S., Fuller, T.K., 2007. Interplay of sediment supply, river incision, and channel morphology revealed by the transient evolution of an experimental bedrock channel. J. Geophys. Res. Earth Surf. 112 (F3).
Fletcher, R.C., Buss, H.L., Brantley, S.L., 2006. A spheroidal weathering model coupling porewater chemistry to soil thicknesses during steady-state denudation. Earth Planet. Sci. Lett. 244 (1), 444–457.
Field, C.B., Behrenfeld, M.J., Randerson, J.T., Falkowski, P., 1998. Primary production of the biosphere: integrating terrestrial and oceanic components. Science 281 (5374), 237–240.
Gabet, E.J., Mudd, S.M., 2010. Bedrock erosion by root fracture and tree throw: a coupled biogeomorphic model to explore the humped soil production function and the persistence of hillslope soils. J. Geophys. Res. Earth Surf. 115 (F4).
Gabet, E.J., Reichman, O.J., Seabloom, E.W., 2003. The effects of bioturbation on soil processes and sediment transport. Annu. Rev. Earth Planet. Sci. 31 (1), 249–273.
Gallen, S.F., Wegmann, K.W., Frankel, K.L., Hughes, S., Lewis, R.Q., Lyons, N., Witt, A.C., 2011. Hillslope response to knickpoint migration in the Southern Appalachians: implications for the evolution of post-orogenic landscapes. Earth Surf. Process. Landf. 36 (9), 1254–1267.
Gillespie, P.A., Howard, C.B., Walsh, J.J., Watterson, J., 1993. Measurement and characterisation of spatial distributions of fractures. Tectonophysics 226 (1), 113–141.
Girard, L., Gruber, S., Weber, S., Beutel, J., 2013. Environmental controls of frost cracking revealed through in situ acoustic emission measurements in steep bedrock. Geophys. Res. Lett. 40 (9), 1748–1753.
Glicken, H., 1996. Rockslide-debris avalanche of May 18, 1980, Mount St. Helens Volcano, Washington (No. 96–677). US Geological Survey.
Gómez-Plaza, A., Martınez-Mena, M., Albaladejo, J., Castillo, V.M., 2001. Factors regulating spatial distribution of soil water content in small semiarid catchments. J. Hydrol. 253 (1), 211–226.
Gomi, T., Sidle, R.C., Richardson, J.S., 2002. Understanding processes and downstream linkages of headwater systems. Bioscience 52 (10), 905–916.
Grady, D.E., Kipp, M.E., 1987. Dynamic rock fragmentation. Fracture Mechanics of Rock Vol. 10, p. 429.
Hahm, W.J., Riebe, C.S., Lukens, C.E., Araki, S., 2014. Bedrock composition regulates mountain ecosystems and landscape evolution. Proc. Natl. Acad. Sci. 111 (9), 3338–3343.
Hales, T.C., Roering, J.J., 2005. Climate-controlled variations in scree production, Southern Alps, New Zealand. Geology 33 (9), 701–704.
Hales, T.C., Roering, J.J., 2007. Climatic controls on frost cracking and implications for the evolution of bedrock landscapes. J. Geophys. Res. Earth Surf. 112 (F2).
Heimsath, A.M., Dietrich, W.E., Nishiizumi, K., Finkel, R.C., 1997. The soil production function and landscape equilibrium. Nature 388 (6640), 358–361.
Heimsath, A.M., Chappell, J., Dietrich, W.E., Nishiizumi, K., Finkel, R.C., 2000. Soil production on a retreating escarpment in southeastern Australia. Geology 28 (9), 787–790.
Heimsath, A.M., DiBiase, R.A., Whipple, K.X., 2012. Soil production limits and the transition to bedrock-dominated landscapes. Nat. Geosci. 5 (3), 210–214.
Heller, P.L., Beland, P.E., Humphrey, N.F., Konrad, S.K., Lynds, R.M., McMillan, M.E., Furbish, D.J., 2001. Paradox of downstream fining and weathering-rind formation in the lower Hoh River, Olympic Peninsula, Washington. Geology 29 (11), 971–974.
Howard, A.D., 1980. Thresholds in river regimes. Thresholds in Geomorphology, pp. 227–258.
Howard, A.D., 1998. Long profile development of bedrock channels: Interaction of weathering, mass wasting, bed erosion, and sediment transport. Geophysical Monograph-American Geophysical Union Vol. 107, pp. 297–319.
Hooke, R.L., 2000. On the history of humans as geomorphic agents. Geology 28 (9), 843–846.
Hurst, M.D., Mudd, S.M., Walcott, R., Attal, M., Yoo, K., 2012. Using hilltop curvature to derive the spatial distribution of erosion rates. J. Geophys. Res. Earth Surf. 117 (F2).
Ibbeken, H., 1983. Jointed source rock and fluvial gravels controlled by Rosin's law: a grain-size study in Calabria, South Italy. J. Sediment. Res. 53 (4).
Isherwood, D., Street, A., 1976. Biotite-induced grussification of the Boulder Creek Granodiorite, Boulder County, Colorado. Geol. Soc. Am. Bull. 87 (3), 366–370.
International Society for Rock Mechanics, 1978. Suggested methods for determining tensile strength of rock materials. Int. J. Rock Mech. Min. Sci. 21, 145–153.
Issa, O.M., Bissonnais, Y.L., Planchon, O., Favis-Mortlock, D., Silvera, N., Wainwright, J., 2006. Soil detachment and transport on field- and laboratory-scale interrill areas: erosion processes and the size-selectivity of eroded sediment. Earth Surf. Process. Landf. 31 (8), 929–939.
Johnson, J.P., 2014. A surface roughness model for predicting alluvial cover and bed load transport rate in bedrock channels. J. Geophys. Res. Earth Surf. 119 (10), 2147–2173.
Johnson, J.P., Whipple, K.X., Sklar, L.S., Hanks, T.C., 2009. Transport slopes, sediment cover, and bedrock channel incision in the Henry Mountains, Utah. J. Geophys. Res. Earth Surf. 114 (F2).
Jomelli, V., Francou, B., 2000. Comparing the characteristics of rockfall talus and snow avalanche landforms in an Alpine environment using a new methodological approach: Massif des Ecrins, French Alps. Geomorphology 35 (3), 181–192.
Kim, B.H., Cai, M., Kaiser, P.K., Yang, H.S., 2007. Estimation of block sizes for rock masses with non-persistent joints. Rock Mech. Rock. Eng. 40 (2), 169–192. http://dx.doi.org/10.1007/s00603-006-0093-8.
Kodama, Y., 1994. Downstream changes in the lithology and grain size of fluvial gravels, the Watarase River, Japan: evidence of the role of abrasion in downstream fining. J. Sediment. Res. 64 (1).
Krumbein, W.C., Tisdel, F.W., 1940. Size distribution of source rocks of sediments. Am. J. Sci. 238 (4), 296–305.
Larsen, I.J., Almond, P.C., Eger, A., Stone, J.O., Montgomery, D.R., Malcolm, B., 2014. Rapid soil production and weathering in the Southern Alps, New Zealand. Science 343 (6171), 637–640.
Lenzi, M.A., Mao, L., Comiti, F., 2004. Magnitude-frequency analysis of bed load data in an Alpine boulder bed stream. Water Resour. Res. 40 (7).
Lukens, C.E., Riebe, C.S., Sklar, L.S., Shuster, D.L., 2015. If rocks could talk: Origin stories told by apatite helium ages and cosmogenic nuclides. Eos Trans. AGU 95 (52) (Fall Suppl., Abstract EP41C-0946).
Mackey, B.H., Roering, J.J., 2011. Sediment yield, spatial characteristics, and the long-term evolution of active earthflows determined from airborne LiDAR and historical aerial photographs, Eel River, California. Geol. Soc. Am. Bull. 123 (7–8), 1560–1576.
Maher, K., Chamberlain, C.P., 2014. Hydrologic regulation of chemical weathering and the geologic carbon cycle. Science 343 (1502). http://dx.doi.org/10.1126/science.1250770.
Marshall, J.A., Sklar, L.S., 2012. Mining soil databases for landscape-scale patterns in the abundance and size distribution of hillslope rock fragments. Earth Surf. Process. Landf. 37 (3), 287–300.
Marshall, J.A., Roering, J.J., 2014. Diagenetic variation in the Oregon Coast Range: implications for rock strength, soil production, hillslope form, and landscape evolution. J. Geophys. Res. Earth Surf. 119 (6), 1395–1417.
Marshall, J.A., Roering, J.J., Bartlein, P.J., Gavin, D.G., Granger, D.E., Rempel, A.W., Praskievicz, S.J., Hales, T.C., 2015. Frost for the trees: Did climate increase erosion in unglaciated landscapes during the late Pleistocene? Sci. Adv. 1 (10), e1500715.
Martel, S.J., 2006. Effect of topographic curvature on near-surface stresses and application to sheeting joints. Geophys. Res. Lett. 33 (1).
Martin, P.M., Mills, A.A., 1977. Does the lunar regolith follow Rosin's law? Moon 16 (2), 215–219.
Matsuoka, N., Murton, J., 2008. Frost weathering: recent advances and future directions. Permafr. Periglac. Process. 19 (2), 195–210.
McFadden, L.D., Eppes, M.C., Gillespie, A.R., Hallet, B., 2005. Physical weathering in arid landscapes due to diurnal variation in the direction of solar heating. Geol. Soc. Am. Bull. 117 (1–2), 161–173.
McGrath, G.S., Nie, Z., Dyskin, A., Byrd, T., Jenner, R., Holbeche, G., Hinz, C., 2013. In situ fragmentation and rock particle sorting on arid hills. J. Geophys. Res. Earth Surf. 118 (1), 17–28.
Menting, F., Langston, A.L., Temme, A.J., 2015. Downstream fining, selective transport, and hillslope influence on channel bed sediment in mountain streams, Colorado Front Range, USA. Geomorphology 239, 91–105.
Michaelides, K., Martin, G.J., 2012. Sediment transport by runoff on debris-mantled dryland hillslopes. J. Geophys. Res. Earth Surf. 117 (F3).
Miller, J.P., 1958. High Mountain Streams: Effects of Geology on Channel Characteristics and Bed Material. State Bureau of Mines and Mineral Resources, New Mexico Institute of Mining and Technology, Albuquerque, NM.
Miller, D.J., Dunne, T., 1996. Topographic perturbations of regional stresses and consequent bedrock fracturing. J. Geophys. Res. Solid Earth 101 (B11), 25523–25536.
Miller, K.L., Szabó, T., Jerolmack, D.J., Domokos, G., 2014. Quantifying the significance of abrasion and selective transport for downstream fluvial grain size evolution. J. Geophys. Res. Earth Surf. 119 (11), 2412–2429.
Milodowski, D.T., Mudd, S.M., Mitchard, E.T.A., 2015. Topographic roughness as a signature of the emergence of bedrock in eroding landscapes. Earth Surf. Dyn. 3, 483–499. http://dx.doi.org/10.5194/esurf-3-483-2015.
Misra, R.K., Gibbons, A.K., 1996. Growth and morphology of eucalypt seedling-roots, in relation to soil strength arising from compaction. Plant Soil 182 (1), 1–11.
Molnar, P., Anderson, R.S., Anderson, S.P., 2007. Tectonics, fracturing of rock, and erosion. J. Geophys. Res. Earth Surf. 112 (F3).
Montgomery, D.R., 2007. Soil erosion and agricultural sustainability. Proc. Natl. Acad. Sci. 104 (33), 13268–13272.
Montgomery, D.R., Brandon, M.T., 2002. Topographic controls on erosion rates in tectonically active mountain ranges. Earth Planet. Sci. Lett. 201 (3), 481–489.
Montgomery, D.R., Buffington, J.M., 1997. Channel-reach morphology in mountain drainage basins. Geol. Soc. Am. Bull. 109 (5), 596–611.

Please cite this article as: Sklar, L.S., et al., The problem of predicting the size distribution of sediment supplied by hillslopes to rivers, Geomorphology (2016), http://dx.doi.org/10.1016/j.geomorph.2016.05.005

Mudd, S.M., Furbish, D.J., 2006. Using chemical tracers in hillslope soils to estimate the importance of chemical denudation under conditions of downslope sediment transport. J. Geophys. Res. Earth Surf. 111 (F2).
Murton, J.B., Peterson, R., Ozouf, J.C., 2006. Bedrock fracture by ice segregation in cold regions. Science 314 (5802), 1127–1129.
National Research Council, 2010. Landscapes on the Edge: New Horizons for Research on Earth's Surface. The National Academies Press, Washington, D.C.
Neal, A., 2004. Ground-penetrating radar and its use in sedimentology: principles, problems and progress. Earth Sci. Rev. 66 (3), 261–330.
Nelson, P.A., Seminara, G., 2011. Modeling the evolution of bedrock channel shape with erosion from saltating bed load. Geophys. Res. Lett. 38 (17).
Newman, D.K., Banfield, J.F., 2002. Geomicrobiology: how molecular-scale interactions underpin biogeochemical systems. Science 296 (5570), 1071–1077.
Norton, K.P., Molnar, P., Schlunegger, F., 2014. The role of climate-driven chemical weathering on soil production. Geomorphology 204, 510–517.
Oberlander, T.M., 1972. Morphogenesis of granitic boulder slopes in the Mojave Desert, California. J. Geol. 1–20.
O'Connor, J.E., Mangano, J.F., Anderson, S.W., Wallick, J.R., Jones, K.L., Keith, M.K., 2014. Geologic and physiographic controls on bed-material yield, transport, and channel morphology for alluvial and bedrock rivers, western Oregon. Geol. Soc. Am. Bull. B30831.
Ouimet, W.B., Whipple, K.X., Granger, D.E., 2009. Beyond threshold hillslopes: channel adjustment to base-level fall in tectonically active mountain ranges. Geology 37 (7), 579–582.
Palmstrom, A., 2005. Measurements of and correlations between block size and rock quality designation (RQD). Tunn. Undergr. Space Technol. 20, 362–377.
Paola, C., Parker, G., Seal, R., Sinha, S.K., Southard, J.B., Wilcock, P.R., 1992. Downstream fining by selective deposition in a laboratory flume. Science 258, 1757.
Parker, G., Wilcock, P.R., Paola, C., Dietrich, W.E., Pitlick, J., 2007. Physical basis for quasi-universal relations describing bankfull hydraulic geometry of single-thread gravel bed rivers. J. Geophys. Res. Earth Surf. 112 (F4).
Parsekian, A.D., Singha, K., Minsley, B.J., Holbrook, W.S., Slater, L., 2015. Multiscale geophysical imaging of the critical zone. Rev. Geophys. 53 (1), 1–26.
Pawlik, Ł., 2013. The role of trees in the geomorphic system of forested hillslopes—a review. Earth Sci. Rev. 126, 250–265.
Pedersen, K., 2000. Exploration of deep intraterrestrial microbial life: current perspectives. FEMS Microbiol. Lett. 185 (1), 9–16.
Perfect, E., 1997. Fractal models for the fragmentation of rocks and soils: a review. Eng. Geol. 48 (3), 185–198.
Poesen, J., Lavee, H., 1994. Rock fragments in top soils: significance and processes. Catena 23 (1), 1–28.
Poesen, J., Van Wesemael, B., Govers, G., Martinez-Fernandez, J., Desmet, P., Vandaele, K., Degraer, G., 1997. Patterns of rock fragment cover generated by tillage erosion. Geomorphology 18 (3), 183–197.
Pollard, D.D., Aydin, A., 1988. Progress in understanding jointing over the past century. Geol. Soc. Am. Bull. 100 (8), 1181–1204.
Posadas, A.N., Giménez, D., Bittelli, M., Vaz, C.M., Flury, M., 2001. Multifractal characterization of soil particle-size distributions. Soil Sci. Soc. Am. J. 65 (5), 1361–1367.
Putkonen, J., Morgan, D., Balco, G., 2014. Boulder weathering in McMurdo Dry Valleys, Antarctica. Geomorphology 219, 192–199.
Rădoane, M., Rădoane, N., Dumitriu, D., Miclăuş, C., 2008. Downstream variation in bed sediment size along the East Carpathian rivers: evidence of the role of sediment sources. Earth Surf. Process. Landf. 33 (5), 674–694.
Rathburn, S., Wohl, E., 2003. Predicting fine sediment dynamics along a pool-riffle mountain channel. Geomorphology 55 (1), 111–124.
Rickenmann, D., Recking, A., 2011. Evaluation of flow resistance in gravel-bed rivers through a large field data set. Water Resour. Res. 47 (7).
Riebe, C.S., Kirchner, J.W., Granger, D.E., Finkel, R.C., 2000. Erosional equilibrium and disequilibrium in the Sierra Nevada, inferred from cosmogenic 26Al and 10Be in alluvial sediment. Geology 28 (9), 803–806.
Riebe, C.S., Kirchner, J.W., Granger, D.E., Finkel, R.C., 2001. Strong tectonic and weak climatic control of long-term chemical weathering rates. Geology 29 (6), 511–514.
Riebe, C.S., Kirchner, J.W., Finkel, R.C., 2004. Erosional and climatic effects on long-term chemical weathering rates in granitic landscapes spanning diverse climate regimes. Earth Planet. Sci. Lett. 224 (3), 547–562.
Riebe, C.S., Sklar, L.S., Overstreet, B.T., Wooster, J.K., 2014. Optimal reproduction in salmon spawning substrates linked to grain size and fish length. Water Resour. Res. 50 (2), 898–918.
Riebe, C.S., Sklar, L.S., Lukens, C.E., Shuster, D.L., 2015. Climate and topography control the size of sediment produced on mountain slopes. Proc. Natl. Acad. Sci. http://dx.doi.org/10.1073/pnas.1503567112.
Riggins, S.G., Anderson, R.S., Anderson, S.P., Tye, A.M., 2011. Solving a conundrum of a steady-state hilltop with variable soil depths and production rates, Bodmin Moor, UK. Geomorphology 128 (1), 73–84.
Roering, J.J., Kirchner, J.W., Dietrich, W.E., 1999. Evidence for nonlinear, diffusive sediment transport on hillslopes and implications for landscape morphology. Water Resour. Res. 35 (3), 853–870.
Roering, J.J., Marshall, J., Booth, A.M., Mort, M., Jin, Q., 2010. Evidence for biotic controls on topography and soil production. Earth Planet. Sci. Lett. 298 (1), 183–190.
Rosin, P., Rammler, E., 1933. The laws governing the fineness of powdered coal. J. Inst. Fuel 7 (29).
Roy, S.G., Johnson, S.E., Koons, P.O., Jin, Z., 2012. Fractal analysis and thermal-elastic modeling of a subvolcanic magmatic breccia: the role of post-fragmentation partial melting and thermal fracture in clast size distributions. Geochem. Geophys. Geosyst. 13 (5).
Shakesby, R.A., Doerr, S.H., 2006. Wildfire as a hydrological and geomorphological agent. Earth Sci. Rev. 74 (3), 269–307.
Sharmeen, S., Willgoose, G.R., 2006. The interaction between armouring and particle weathering for eroding landscapes. Earth Surf. Process. Landf. 31 (10), 1195–1210.
Silver, W.L., Neff, J., McGroddy, M., Veldkamp, E., Keller, M., Cosme, R., 2000. Effects of soil texture on belowground carbon and nutrient storage in a lowland Amazonian forest ecosystem. Ecosystems 3 (2), 193–209.
Sklar, L.S., Dietrich, W.E., 2001. Sediment and rock strength controls on river incision into bedrock. Geology 29 (12), 1087–1090.
Sklar, L.S., Dietrich, W.E., 2004. A mechanistic model for river incision into bedrock by saltating bed load. Water Resour. Res. 40 (6).
Sklar, L.S., Dietrich, W.E., 2006. The role of sediment in controlling steady-state bedrock channel slope: implications of the saltation–abrasion incision model. Geomorphology 82 (1), 58–83.
Sklar, L.S., Dietrich, W.E., Foufoula-Georgiou, E., Lashermes, B., Bellugi, D., 2006. Do gravel bed river size distributions record channel network structure? Water Resour. Res. 42 (6).
Smith, G.H., Nicholas, A.P., Ferguson, R.I., 1997. Measuring and defining bimodal sediments: problems and implications. Water Resour. Res. 33 (5), 1179–1185.
Stallard, R.F., 1995. Tectonic, environmental, and human aspects of weathering and erosion: a global review from a steady-state perspective. Annu. Rev. Earth Planet. Sci. 23, 11–40.
Struck, M., Andermann, C., Hovius, N., Korup, O., Turowski, J.M., Bista, R., Pandit, H.P., Dahal, R.K., 2015. Monsoonal hillslope processes determine grain size-specific suspended sediment fluxes in a trans-Himalayan river. Geophys. Res. Lett. 42 (7), 2302–2308.
Strudley, M.W., Murray, A.B., Haff, P.K., 2006. Regolith thickness instability and the formation of tors in arid environments. J. Geophys. Res. Earth Surf. 111 (F3).
Tetegan, M., Pasquier, C., Besson, A., Nicoullaud, B., Bouthier, A., Bourennane, H., Desbourdes, C., King, D., Cousin, I., 2012. Field-scale Estimation of the Volume Percentage of Rock Fragments in Stony Soils by Electrical Resistivity. In. pp. 67–74.
Thomas, D.N., Dieckmann, G.S., 2002. Antarctic sea ice—a habitat for extremophiles. Science 295 (5555), 641–644.
Turcotte, D.L., 1986. Fractals and fragmentation. J. Geophys. Res. Solid Earth 91 (B2), 1921–1926.
Turowski, J.M., Rickenmann, D., 2009. Tools and cover effects in bedload transport observations in the Pitzbach, Austria. Earth Surf. Process. Landf. 34 (1), 26–37.
Wakasa, S.A., Nishimura, S., Shimizu, H., Matsukura, Y., 2012. Does lightning destroy rocks?: results from a laboratory lightning experiment using an impulse high-current generator. Geomorphology 161, 110–114.
Walder, J., Hallet, B., 1985. A theoretical model of the fracture of rock during freezing. Geol. Soc. Am. Bull. 96 (3), 336–346.
Webb, R.H., Pringle, P.T., Reneau, S.L., Rink, G.R., 1988. Monument Creek debris flow, 1984: implications for formation of rapids on the Colorado River in Grand Canyon National Park. Geology 16 (1), 50–54.
Weibull, W., 1951. A statistical distribution function of wide applicability. J. Appl. Mech 103, 33.
Wells, T., Willgoose, G.R., Hancock, G.R., 2008. Modeling weathering pathways and processes of the fragmentation of salt weathered quartz-chlorite schist. J. Geophys. Res. Earth Surf. 113 (F1).
West, A.J., Galy, A., Bickle, M., 2005. Tectonic and climatic controls on silicate weathering. Earth Planet. Sci. Lett. 235 (1), 211–228.
White, A.F., Blum, A.E., 1995. Effects of climate on chemical_ weathering in watersheds. Geochim. Cosmochim. Acta 59 (9), 1729–1747.
Whitney, J.W., Harrington, C.D., 1993. Relict colluvial boulder deposits as paleoclimatic indicators in the Yucca Mountain region, southern Nevada. Geol. Soc. Am. Bull. 105 (8), 1008–1018.
Whittaker, A.C., Attal, M., Cowie, P.A., Tucker, G.E., Roberts, G.P., 2008. Decoding temporal and spatial patterns of fault uplift using transient river long profiles. Geomorphology 100, 506–526. http://dx.doi.org/10.1016/j.geomorph.2008.01.018.
Whittaker, A.C., Attal, M., Allen, P.A., 2010. Characterizing the origin, nature and fate of sediment exported from catchments perturbed by active tectonics. Basin Res. 22, 809–828. http://dx.doi.org/10.1111/j.1365–2117.2009.00447.x.
Wieczorek, G.F., Snyder, J.B., Waitt, R.B., Morrissey, M.M., Uhrhammer, R.A., Harp, E.L., Finewood, L.G., 2000. Unusual July 10, 1996, rock fall at Happy Isles, Yosemite National Park, California. Geol. Soc. Am. Bull. 112 (1), 75–85.
Wines, D.R., Lilly, P.A., 2002. Measurement and analysis of rock mass discontinuity spacing and frequency in part of the Fimiston Open Pit operation in Kalgoorlie, Western Australia: a case study. Int. J. Rock Mech. Min. Sci. 39 (5), 589–602.
Wohl, E., 2004. Limits of downstream hydraulic geometry. Geology 32 (10), 897–900.
Wolcott, J., 1988. Nonfluvial control of bimodal grain-size distributions in river-bed gravels. J. Sediment. Res. 58 (6).
Vericat, D., Batalla, R.J., Garcia, C., 2006. Breakup and reestablishment of the armour layer in a large gravel-bed river below dams: the lower Ebro. Geomorphology 76 (1), 122–136.
Yoo, K., Mudd, S.M., 2008. Discrepancy between mineral residence time and soil age: Implications for the interpretation of chemical weathering rates. Geology 36 (1), 35–38.
Ziegler, M., Loew, S., Moore, J.R., 2013. Distribution and inferred age of exfoliation joints in the Aar Granite of the central Swiss Alps and relationship to Quaternary landscape evolution. Geomorphology 201, 344–362.
Zimmer, V.L., Collins, B.D., Stock, G.M., Sitar, N., 2012. Rock fall dynamics and deposition: an integrated analysis of the 2009 Ahwiyah Point rock fall, Yosemite National Park, USA. Earth Surf. Process. Landf. 37 (6), 680–691.
Zwieniecki, M.A., Newton, M., 1994. Root distribution of 12-year-old forests at rocky sites in southwestern Oregon: effects of rock physical properties. Can. J. For. Res. 24 (9), 1791–1796.

Please cite this article as: Sklar, L.S., et al., The problem of predicting the size distribution of sediment supplied by hillslopes to rivers, Geomorphology (2016), http://dx.doi.org/10.1016/j.geomorph.2016.05.005